A NONLINEAR TRANSISTOR MODEL AND DEVICE CHARACTERIZATION

by

PARVIZ KIANKHOOY-FARD

B. S., Missouri University, 1963

A MASTER'S REPORT

submitted in partial fulfillment of the

requirements for the degree

MASTER OF SCIENCE

Department of Electrical Engineering

KANSAS STATE UNIVERSITY
Manhattan, Kansas

1966

Approved by:

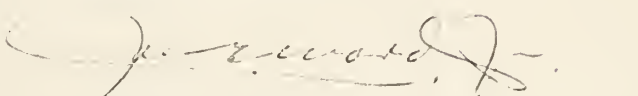

Major Professor

TABLE OF CONTENTS

1. INTRODUCTION

As the requirements for computer circuit performance becomes more demanding, there is an ever increasing need for a more efficient method of describing transistor circuits. Before this need can be met, a transistor model must be available which will permit accurate prediction.

There are numerous models available which (3) permit accurate prediction. Many parameters associated with these models are not easily evaluated, and the evaluations often require facilities and measurement techniques which are not commonly available. These models cannot be easily simulated on the computer; such a simulation often requires advanced type computer, and program execution times are lengthy. In short, these models are cumbersome to use in practice. There is need for a model which is based on theoretical principles but which can be easily used in practice. Such a model 1) should be a good compromise between accuracy and tractibility, 2) should have the property of ease of evaluation of its parameters with conventional facilities and reasonable precision, 3) should permit simulation on the computer easily with a reasonable execution time, 4) should be valid for large as

well as small imput signals. Large signal input can be as large as to derive the transistor into saturation, but should not be so large to cause high injection effects.

The model to be described in this report is not a complex model. In fact, it has been around for quite some time. However, with the addition of the nonlinear characteristics and with careful device characterization, this model can provide the necessary means of predicting response to large as well as small input signal.

The characteristics of the p-n junction have been studied by many authors (2). By concentrating study on only one junction, one can understand more readily some of the more important transistor characteristics. In developing this model, each junction of a common base transistor is studied, while the other terminal is shorted to base. The use of superposition is made in obtaining the model. Because the model is nonlinear, the use of superposition may at first be considered invalid. The model is to be simulated on the computer, and the computer obtains the solution to the differential equations by means of numerical integration. By choosing small enough intervals of integration, nonlinearity can be observed as linearity within each interval. The program re-evaluates the nonlinear elements for each given interval. Then using the system of

nonlinear differential equations describing the model, in conjunction with the internal subprograms, the value of the voltages corresponding to that interval are predicted and corrected. If the predicted value is not within specified allowable error from the corrected value, then the program modifies the interval of integration and repeats the cycle until the specified allowable error is met. Thus use of superposition is validated.

Most of the methods described in this report to evaluate the parameters of the model are standard methods; however, they are modified when necessary.

Although the model is tested with fast rise-time input pulses, the model has more general applications. The input pulse tests are more severe than simple a-c or d-c input tests. By fourier-series expansion it can be shown that the pulse has both a-c and d-c components.

2. EQUIVALENT CIRCUIT

The model being derived is based on the Ebers and Moll's equations for transistors (1), Equation (1) and (2). The direction of the currents and polarity of the voltage terminals are shown in Fig. (1).

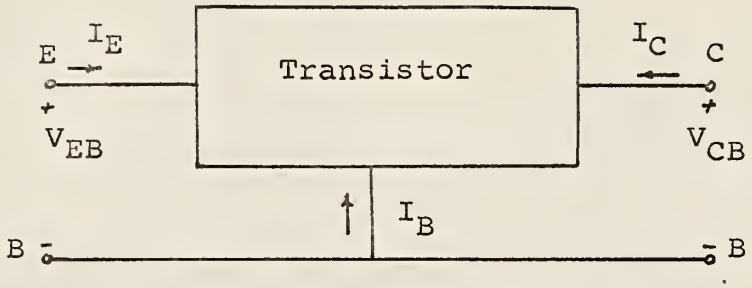

Fig. 1. The direction of current and polarity of the voltage which corresponds to Equations (1) and (2).

Where:

I_E = Emitter Current
I_C = Collector Current
V_E = Emitter-to-Base Voltage
V_C = Collector-to-Base Voltage

$$I_E = a_{11}(e^{qV_{EB}/kT} - 1) - a_{12}(e^{qV_{CB}/kT} - 1) \qquad (1)$$

$$I_C = a_{21}(e^{qV_{EB}/kT} - 1) - a_{22}(e^{qV_{CB}/kT} - 1) \qquad (2)$$

Where:

q Electron Charge
k Boltzmann's Constant
T Temperature
a_{11}, a_{22}, a_{21}, and a_{12} are Constants

The constants a_{11}, a_{12}, a_{21} and a_{22} are functions of transistor material and junction temperature. The meanings given to these constants in this paper are different from the meanings that are given in the reference (1). This will be further discussed. Equations (1) and (2) are derived solely from the diffusion equation for the d-c condition. The assumptions made in deriving Equations (1) and (2) are: that drift current is negligible compared to diffusion current, and that there are no mobile charges in the depletion layers (7). The above assumptions are valid for the first derived model. The model obtained in this manner will be called the intrinsic model. The intrinsic model will be further completed by introducing some of the extrinsic elements. The extrensic elements considered are: depletion junction capacitance, bulk resistance, and header capacitances. The model resulted by introducing extrinsic elements into intrinsic model is called extrinsic model. The extrinsic model further be completed by introducing additional non-linear elements to the model to account for base width modulation and other effects caused by forward baising collector junction, and this model will be called complete model.

The solution to Equation (1) and (2) for I_E and I_C are obtained by superposition. This is done 1) by setting the

voltage V_{CB}= 0 and obtaining the I_E and I_C only due to V_{EB}; 2) by setting the voltage V_{EB}= 0 and obtaining the I_E and I_C only due to V_{CE}; 3) the I_E and I_C that satisfies equations (1) and (2) are the summation of I_E's obtained from condition (1) and (2) and summation of I_C's obtained from condition (1) and (2).

The value of V_{CB} is set equal to zero by shorting the collector to base. The equations (1) and (2) are then reduced to equations (3) and (4) respectively.

$$I_{E1} = a_{11}(e^{qV_{EB}/kT} - 1) \qquad (3)$$

$$I_{C1} = a_{21}(e^{qV_{EB}/kT} - 1) \qquad (4)$$

Equation (3) is analogous to the voltage v.s. current characteristics of a p-n junction diode. The current-voltage characteristics of a p-n junction can be represented by equation (5).

$$I = I_s\ (e^{qV/kT} - 1) \qquad (5)$$

where:

I_s back saturation current of a p-n junction.

I_S is function of cross sectional junction area, diffusion constant, diffusion length and dopping of acceptors and holes in p region and n region.

A close comparison between equations (3) and (5) yields that constant a_{11} is some sort of back saturation current of a p-n junction. So a_{11} will be defined as I_{SE}, the back saturation current of the emitter-to-base junction when the collector is shorted to base. By substituting I_{SE} in equation (3), equation (6) is obtained.

$$I_{E1} = I_{SE} \left(e^{qV_{EB}/kT} - 1\right) \tag{6}$$

By Kirchboff's current law:

$$I_E = -(I_C + I_B) \tag{7}$$

By dividing equation (4) into equation (6) a_{21} is obtained, equation (8).

$$a_{21} = \frac{I_{C1}}{I_{E1}} \cdot I_{SE} \tag{8}$$

A_1 is defined as $\frac{I_{C1}}{I_{E1}} = A_1$ (9)

Further manipulation results equation (10).

$$I_{C1} = A_1 I_{SE} \left(e^{qV_{EB}/kT} - 1\right) \qquad (10)$$

Or $I_{C1} = A_1 I_{E1}$

Equations (6) and (11) suggest that the below model can be derived, Fig. (2). The model Fig. (2) suggests that for understanding the behavior or the emitter junction, one can investigate the modified diode of Fig. (2). Hence, the characteristics of the diode will be investigated. The voltage vs. current characteristics of the diode p-n junction is shown in Fig. (3), and for an ideal diode, the functional relationship representing this V-I characteristic is given by equation (12).

The functional relationship describing the conductance of the junction due to the diffusion mechanism is defined in equation (13).

$$G_D = \frac{I}{V} = \frac{I_S\left(e^{\delta V} - 1\right)}{V} \qquad (13)$$

V is applied Voltage.

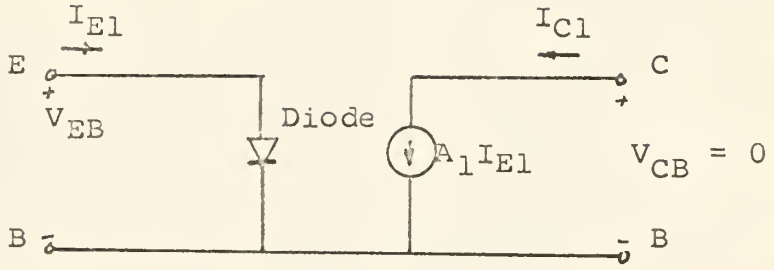

Fig. 2. Model representation of emitter junction when $V_{CB} = 0$.

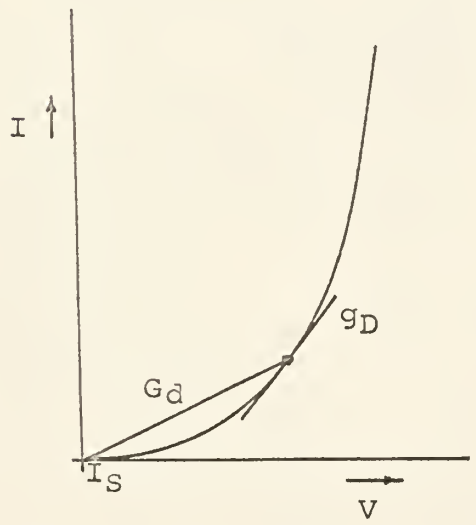

Fig. 3. V-I Characteristic of Diode.

$$I = I_S(e^{V} - 1) \qquad (12)$$

$$= q/kT$$

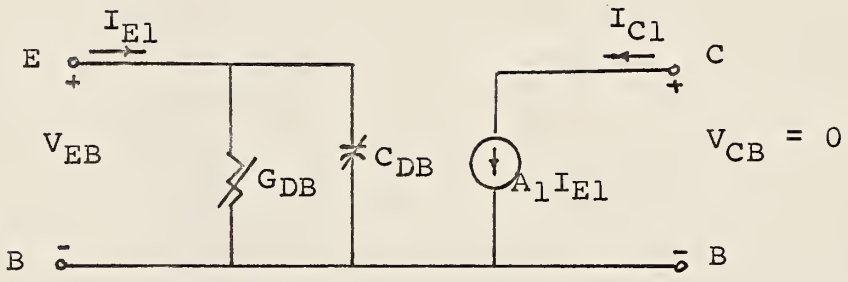

Fig. 4. Model representation of emitter junction with nonlinear elements, when $V_{CB} = 0$.

Where:

$$G_{DB} = \frac{I_{SE}(e^{\gamma V_{EB}} - 1)}{V_{EB}} \tag{15}$$

$$C_{DB} = \gamma_b \, I_{SE} e^{\gamma V_{EB}} \tag{16}$$

The functional relationship describing the diffusion capacitance of the junction is given by equation (14).

$$C_D = \tau_b \frac{dI}{dV} = \tau_b I_S e^{\gamma V} \qquad (14)$$

τ_b the effective minority lifetime in the base.

The model in Fig. (2) can be presented as shown in Fig. (4).

Now, by setting the value of V_{EB} equal to zero in equations (1) and (2), characteristics of the collector junction may be obtained which are similar to the emitter characteristics when $V_{CB} = 0$.

$$I_{E2} = -a_{12}(e^{\mu V_{CB}} - 1) \qquad (17)$$

$$I_{C2} = -a_{22}(e^{\mu V_{CB}} - 1) \qquad (18)$$

$$\mu = q/\kappa T$$

A_2 is defined as $$A_2 = \frac{I_{E2}}{I_{C2}} \qquad (19)$$

A close comparison between equations (5) and (18) yields that constant a_{22} is some sort of back saturation current of a p-n junction. Then a_{22} will be defined as I_{SC}, the back saturation current of the collector to base junction when the emitter is shorted to the base. By substituting

I_{SC} in equation (18), equation (20) is obtained.

$$I_{C2} = -I_{SC}(e^{\mu V_{CB}} - 1) \qquad (20)$$

Further manipulations similar to the manipulation done for the emitter junction yield equations (21-22) for collector junction.

$$I_{C2} = -I_{SC}(e^{\mu V_{CB}} - 1) \qquad (21)$$

$$I_{E2} = A_2 I_{C2} \qquad (22)$$

The equations (21) and (22) suggest that model Fig. (5) can be derived. The model in Fig. (5) can be presented as shown in Fig. (6) by introducing nonlinear elements.

Now the solution to the equations (1) and (2) are:

$$I_E = I_{E1} + I_{E2} \qquad (23)$$

$$I_C = I_{C1} + I_{C2} \qquad (24)$$

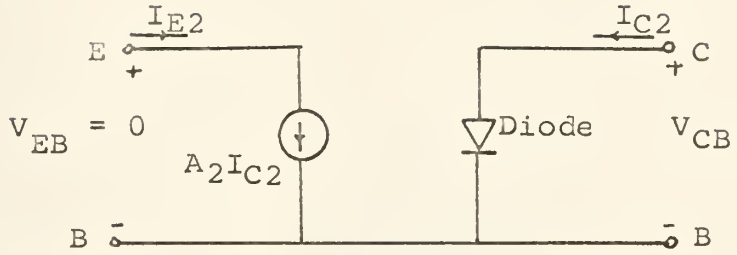

Fig. 5. Model representation of collector junction when $V_{EB} = 0$.

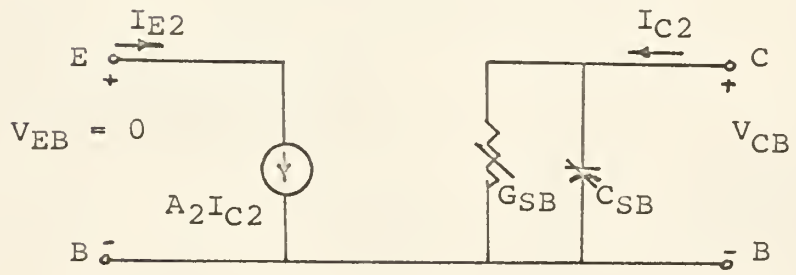

Fig. 6. Model representation of collector junction with nonlinear elements, when $V_{EB} = 0$.

Therefore:

$$I_E = I_{SE}(e^{\gamma V_{EB}} - 1) \qquad (25)$$

$$I_C = A_1 I_{E1} - I_{SC}(e^{\mu V_{CB}} - 1) \qquad (26)$$

Equations (25) and (26) suggest that model in Fig. (7) can be derived. The Model in Fig. (7) can be represented as in Fig. (8) by introducing nonlinear elements.

An equivalent circuit for the common emitter configuration of the equivalent circuit of Fig. (8) will be obtained. The first step is to redraw the circuit of Fig. (8) into a "T" equivalent circuit as shown in Fig. (9). Further manipulations of Fig. (9) suggest the below equations.

$$I_B = I_{E1} + A_2 I_{C2} - A_1 I_{E1} - I_{C2} \qquad (35)$$

$$\text{Or} \quad I_B = -I_{E1}(1 + A_1) - I_{C2}(1 + A_2) \qquad (36)$$

$$\text{And} \quad I_C = A_1 I_{E1} + I_{C2} \qquad (37)$$

$$\text{Or} \quad I_C = I_{C2}(1 - A_2) + I_{C2}A_2 + A_1 I_{E1} \qquad (38)$$

Equations (36) and (37) suggest Fig. (10).

A_1 and A_2 can be related to hFE and hFEI respectively. This is done as follows. The transistor is operated inversely and V_{EB} is set equal to zero.

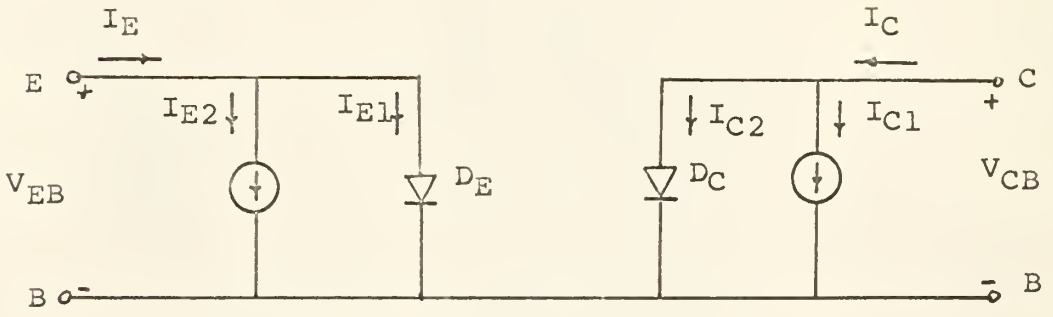

Fig. 7. Model representation of a common base transistor.

$$I_{E1} = I_{SE}(e^{\alpha V_{EB}} - 1) \tag{27}$$

$$I_{C2} = -I_{SC}(e^{\beta V_{CB}} - 1) \tag{28}$$

$$I_{E2} = A_2 I_{C2} \tag{29}$$

$$I_{C1} = A_1 I_{E1} \tag{30}$$

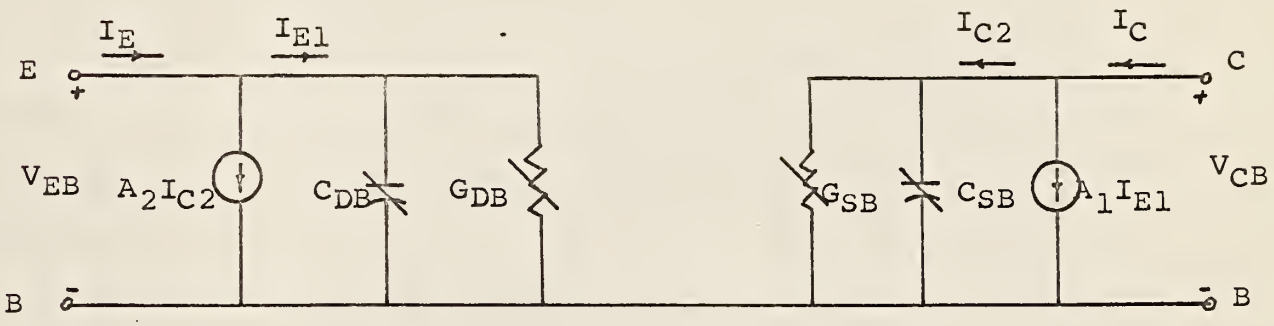

Fig. 8. Intrinsic Model representation of a Common base configuration of transistor with nonlinear elements.

Where:

$$G_{DB} = \frac{I_{SE}(e^{\gamma V_{EB}} - 1)}{V_{EB}}$$

$$C_{DB} = \gamma_b \, I_{SE} e^{\gamma V_{EB}}$$

$$\gamma = q/kT$$

$$G_{SB} = \frac{I_{SC}(e^{\mu V_{CB}} - 1)}{V_{CB}}$$

$$C_{SB} = \gamma_b h_{FE} \, I_{SC} e^{\mu V_{CB}}$$

$$\mu = q/kT$$

hFE - short-circuit current gain for common-emitter mode of transistor operation.

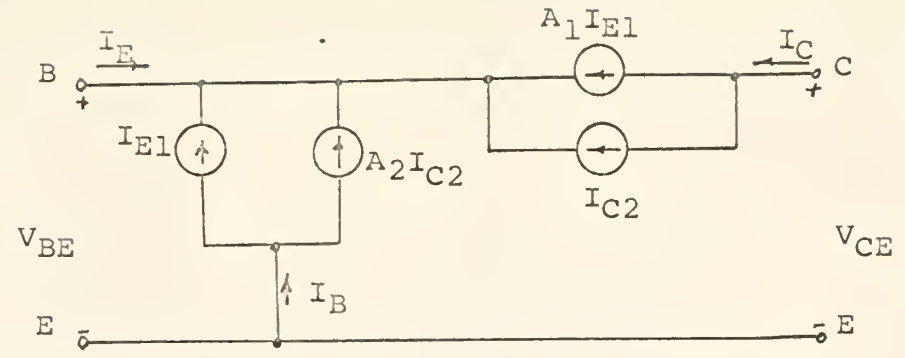

Fig. 9. "T" Equivalent Circuit of Fig. 8.

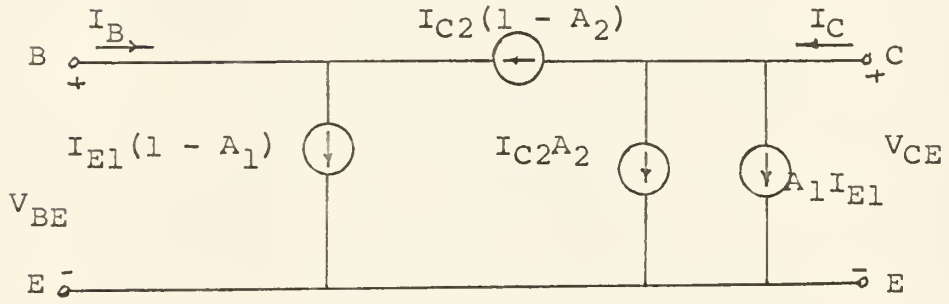

Fig. 10. Intrinsic Common Emitter Equivalent Circuit of Transistor.

$$I_{E1} = I_{SE}(e^{-\delta V_{BE}} - 1) \tag{39}$$

$$I_{C2} = -I_{SC}(e^{\mu(V_{CE} - V_{BE})} - 1) \tag{40}$$

The parameter hFEI is defined as short-circuit common-emitter current gain for a transistor operated inversely.

$$\frac{I_E}{I_B} = hFEI \tag{41}$$

$$A_2 = \frac{I_E}{I_C} \tag{42}$$

$$\text{Or} \quad A_2 = \frac{I_E}{I_E + I_B} \tag{43}$$

$$\text{Or} \quad A_2 = -\frac{1}{1 + \frac{I_B}{I_E}} = -\frac{hFEI}{1 + hFEI} \tag{44}$$

Now V_{CE} is set equal to zero, therefore:

$$\frac{I_C}{I_B} = \frac{A_1}{1 - A_1} = hFE \tag{45}$$

$$\text{Or} \quad A_1 = \frac{hFE}{1 + hFE} \tag{46}$$

The Intrinsic Model representation of a common-emitter configuration of transistor with nonlinear elements is shown in Fig. (11).

The model in Fig. (11) is based on the diffusion mechanism only, and is called an intrinsic model. This model can be further completed by introducing extrinsic elements in the model which are: junction depletion capacitance, bulk resistances, and header capacitance. Although the extrinsic elements are not derived from diffusion equation, they may be dependent on the junction current or junction voltage. This will be discussed.

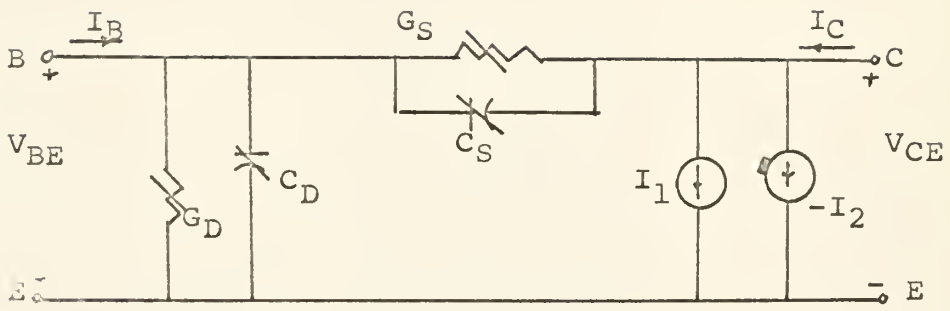

Fig. 11. Intrinsic Model for a Common-Emitter Configuration.

Where:

$$G_D = \frac{I_{SE}(e^{-\gamma V_{BE}} - 1)}{(hFE + 1)V_{BE}} \qquad G_S = \frac{I_{SC}(e^{-\mu(V_{BE} - V_{CE})} - 1)}{(hFEI + 1)(V_{CE} - V_{BE})}$$

$$C_D = \frac{\tau_b I_{SE} e^{-\gamma V_{BE}}}{(hFE + 1)} \qquad C_S = \frac{\tau_b hFE\ e^{-\mu(V_{BE} - V_{CE})}}{(hFEI + 1)}$$

$$I_1 = hFE\ V_{BE} G_D \qquad I_2 = hFEI\ G_S(V_{BE} - V_{CE})$$

The variation of the depletion layer capacitance of the diode p-n junction as a function of the applied voltage depends on the nature of the charge distributed on the junction. This capacitance for the abrupt charge density distribution is in the form of equation (47).

$$C_J = \frac{C_1}{(V\phi - V)^{\frac{1}{2}}} \tag{47}$$

Where: C_1 is a constant function of the dopping level, area of the junction and permittivity of the junction. $V\phi$ is the built-in depletion layer voltage which is a function of semi-conductor material. V is the externally applied voltage across the junction.

The depletion layer capacitances for the linearly graded charge density is in the form of equation (48).

$$C_J = \frac{C_1}{(V\phi - V)^{1/3}} \tag{48}$$

The charge distributions used in the transistor junctions are usually either abrupt or linearly graded. However, they are not ideally abrupt or linearly graded, so that the value m is chosen instead of the powers 1/2 or 1/3 for $(V\phi - V)$.

$$\text{Thus } C_J = \frac{C_1}{(V_\phi - V)^m}$$

It should be pointed out that the assumption was made that there are no mobile carriers in the depletion layer.

The bulk resistance of the emitter region or the collector region is obtained from the conductivity of the emitter region or the collector region respectively. However, these resistances are small enough to be ignored for all practical purposes. The bulk resistances of the base region is not only due to the conductivity of the base region, but also depends on the recombination of the carriers in the base region which is strongly dependent on the magnitude of emitter current. This phenomena is not well understood.

The header capacitances are due to the lead wires to transistor and the transistor encopsilation. These capacitances could affect the performance of the transistor at high speed application.

The model including the extrinsic parameter for the common emitter configuration is shown in Fig. (12).

The functional relationship representing the parameters of Fig. (8) for PNP and NPN transistor are on page of this report.

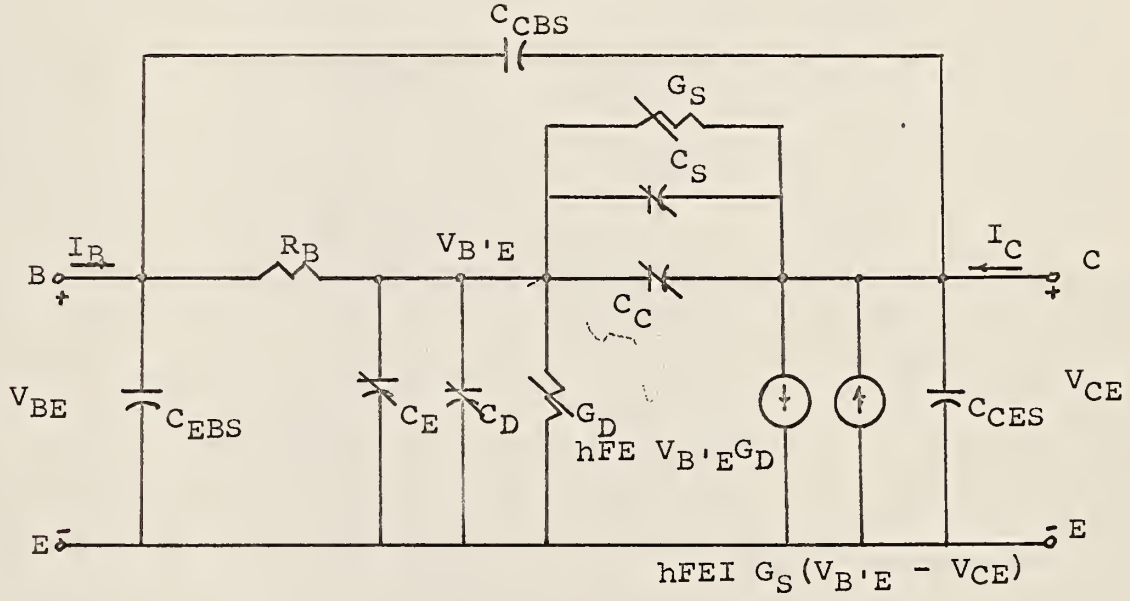

Fig. 12. Extrinsic Model for Common Emitter Configuration.

The parameters corresponding to Fig. (9) for PNP and NPN transistors are given below:

PNP	NPN
$C_E = \frac{C_{E1}}{(V_E - V_{B'E})^m}$	$C_E = \frac{C_{E1}}{(V_{B'E} - V_E)^m}$
$C_C = \frac{C_{C1}}{(V_C - (V_{CE} - V_{B'E}))^n}$	$C_C = \frac{C_{C1}}{((V_{CE} - V_{B'E}) - V_C)^n}$
$C_D = \frac{\gamma_b I_{SE} e^{-\gamma V_{B'E}}}{(h_{FE} + 1)}$	$C_D = \frac{b I_{SE} e^{\gamma V_{B'E}}}{(h_{FE} + 1)}$
$G_D = \frac{I_{SE}(e^{-V_{B'E}} - 1)}{(h_{FE} + 1)V_{B'E}}$	$G_D = \frac{I_{SE}(e^{\gamma V_{B'E}} - 1)}{(h_{FE} + 1)V_{B'E}}$
$C_S = \gamma_b \frac{I_{SC} h_{FE} (e^{-\mu(V_{CE}-V_{B'E})} - 1)}{(h_{FEI} + 1)}$	$C_S = \frac{\gamma_b I_{SC} h_{FE} (e^{\mu(V_{CE}-V_{B'E})} - 1)}{(h_{FEI} + 1)}$
$G_S = \frac{I_{SC}(e^{-\mu(V_{CE}-V_{B'E})} - 1)}{(h_{FEI} + 1)(V_{B'E} - V_{CE})}$	$G_S = \frac{I_{SC}(e^{\mu(V_{CE}-V_{B'E})} - 1)}{(h_{FEI} + 1)(V_{CE} - V_{B'E})}$

C_E Emitter junction depletion capacitance.
C_{E1} The value of C_E when $(V_E - V_{B'E}) = 1$.
m The parameter related to the C_E, evaluated emperically.
C_C, C_{C1}, n Collector parameters which are analogous to the C_E, C_{E1}, and m respectively.
C_D Emitter junction diffusion capacitance.
γ_b The effective minority carrier lifetime in the base. It is a function of q/kT for emitter junction.
I_{SE} Back saturation current for emitter junction.
h_{FE} Short-circuit current gain for common-emitter mode, of normal transistor operation. Equation (45).
$V_{\phi E}$ The barrier potential of the emitter junction.
μ, I_{SC}, $V_{\phi C}$ Collector parameters, which are analogous to the γ, I_{SE}, and $V_{\phi E}$, respectively.
h_{FEI} Short-circuit common-emitter current gain for a transistor operated inversely. Equation (41).

3. DEVICE CHARACTERIZATION

The techniques used to characterize the device will be discussed here. It will become apparent later from the sensitivity studies that not all device parameters discussed will need to be measured on each and every device (5). In practice nominal values will suffice for a given family of devices.

Because of the similarity in which the emitter and collector junctions are represented in the model it is sufficient to describe only the measurements performed on the emitter junction in detail. The few differences that exist in the measurement techniques for the collector are appropriately cited.

The parameter I_{SE} and γ are determined with the emitter biased in the forward direction and the collector shorted to base. The emitter input is a ramp input. Although the value of q/kT is attached to the γ in most device treatises, it is found experimentally that the γ is equal to the $\frac{q}{akT}$ where $\underline{a}$ is experimentally found. The existence of $\underline{a}$ can be explained by the approximation used in evaluating G_D and C_D. Further manipulation of equation (5) reveals equation (50).

$$I_E = I_{SE}(e^{\gamma V} - 1) \qquad (5)$$

Or $$I_E = I_{SE}e^{\gamma V} \qquad e^{\gamma V} \gg 1 \qquad (50)$$

And $$\log_{10} I_E = \log_{10} I_{SE} + V(\gamma \log_{10} e) \qquad (50)$$

The value of I_{SE} then, is obtained by plotting $\log_{10} I_E$ vs. V. The intersection of the extrapolated line with the $\log_{10} I_E$ axis is the value of log I_{SE} and the slope of the line is $\gamma \log_{10} e$. A plot of the V_{EB} vs. I_E is shown in Fig. 14. It is incorrect to use the terminal voltage V_{EB} for the value of V in equation (50), because the V in equation (50) is the intrinsic voltage applied across the junction. The value V in terms of V_{EB} is given in equation (51).

$$V = V_{BE} - I_E R_{SE} \qquad (51)$$

Where R_{SE} is emitter bulk resistance.

The modified V-I characteristic is shown in Fig. (13). The graphical technique used to evaluate γ and I_{SE} for the transistor X is shown in Fig. (14). (See Appendix 1 for information on Transistor X).

The Barrier junction potential $V\phi$ can be evaluated by equation (52).

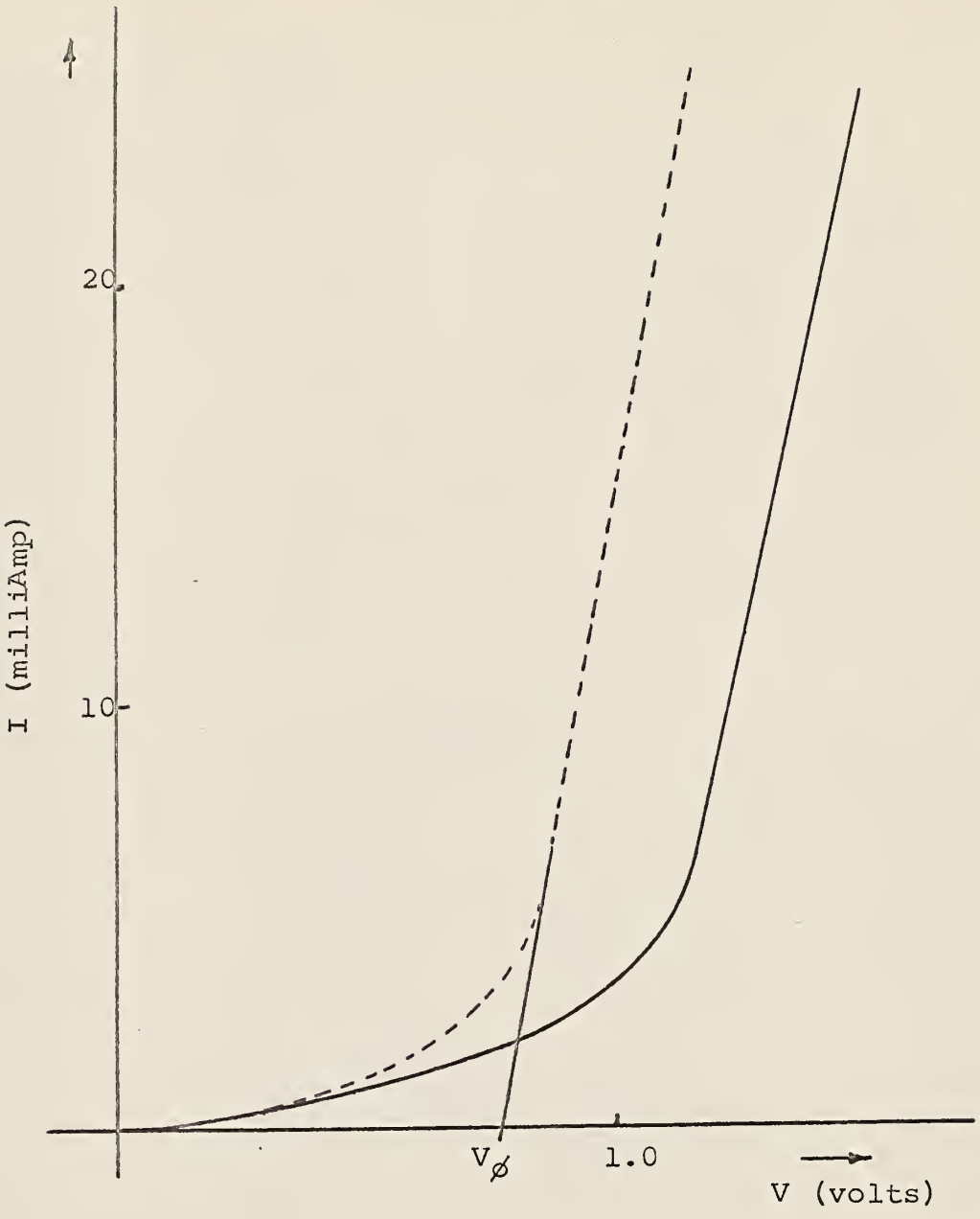

Fig. 13. The Diode V-I Characteristic.

Solid line is terminal voltage v.s. current.
Dash line is corrected value of voltage v.s. current.

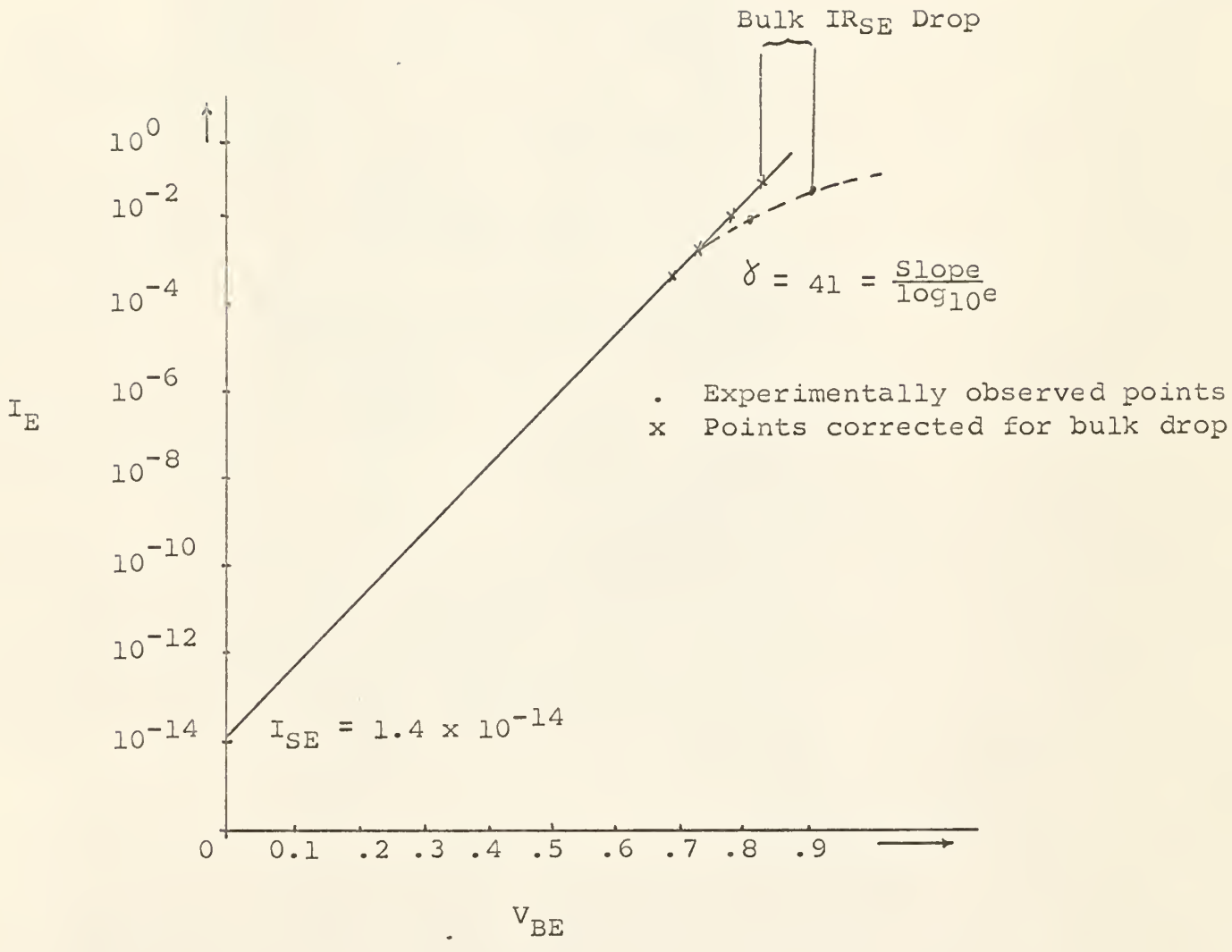

Fig. 14. Graphical technique to evaluate I_{SE} and γ.

$$V\phi = \frac{kT}{q} \ln \frac{NaNd}{Ni^2} \qquad (52)$$

Na = density of acceptor atoms.
Nd = density of donor atoms.
Ni = carrier density in an intrinsic semi-conductor.

Equation (52) is very cumbersome to use in practice. Vø can be evaluated easily by approximation. The sensitivity study has revealed that the Vø is not a very sensitive parameter and a close approximation is accurate enough. A diode at high current can be approximated by a series circuit consisting of a battery equivalent to barrier potential, a resistance which is equivalent to the diffusion resistance of the diode, and an ideal diode. The extrapolation of the slope to the V-I characteristic will meet the V-axis approximately at Value Vø. The graphical evaluation of this barrier potential is shown in Fig. 13. The nominal value of .8 volts can be used for a silicon transistor (5).

C_{El} and m are obtained from capacity measurements on the emitter junction (collector open circuited). The capacitance remaining, after the contribution of the lands and header are removed, versus the true junction voltage is plotted on log-log paper. The junction voltage is the applied voltage less the contribution of the barrier potential. Fig. 15 is an example of how the values of C_{El} and m are obtained.

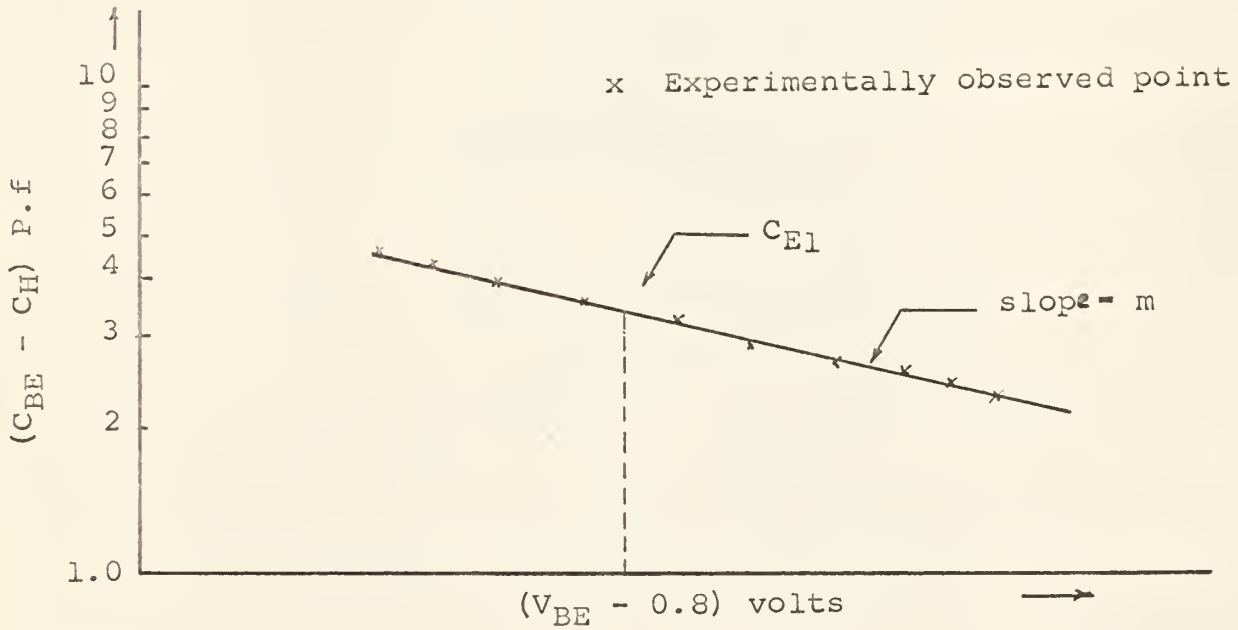

Fig. 15. Graphical technique for obtaining the value m and C_{E1}.

A computer program can be written to evaluate C_{El}, m and Vø simultaneously. This can be done by sequential least square fit, which will find those values of C_{El}, m and Vø to fit experimental data and equation (49).

Short circuit common emitter current gain is measured in the conventional manner. Fig. 16 is an example of the dependency of this parameter on emitter current.

The value of τ_b may be obtained by

$$\tau_b = \frac{1.22}{(1-\alpha_N)\ w_N} \tag{53}$$

Where α_N is low frequency of short circuit current gain for common base circuit.
Where W_N α cut off frequency for the common base short-circuit current gain for a normally operated transistor.

In practice it is cumbersome to use equation (53) for evaluation of τ_b. The charge method technique is more widely used for evaluation τ_b, which is:

$$\tau_b = \frac{\Delta Q_B}{\Delta I_B} \tag{54}$$

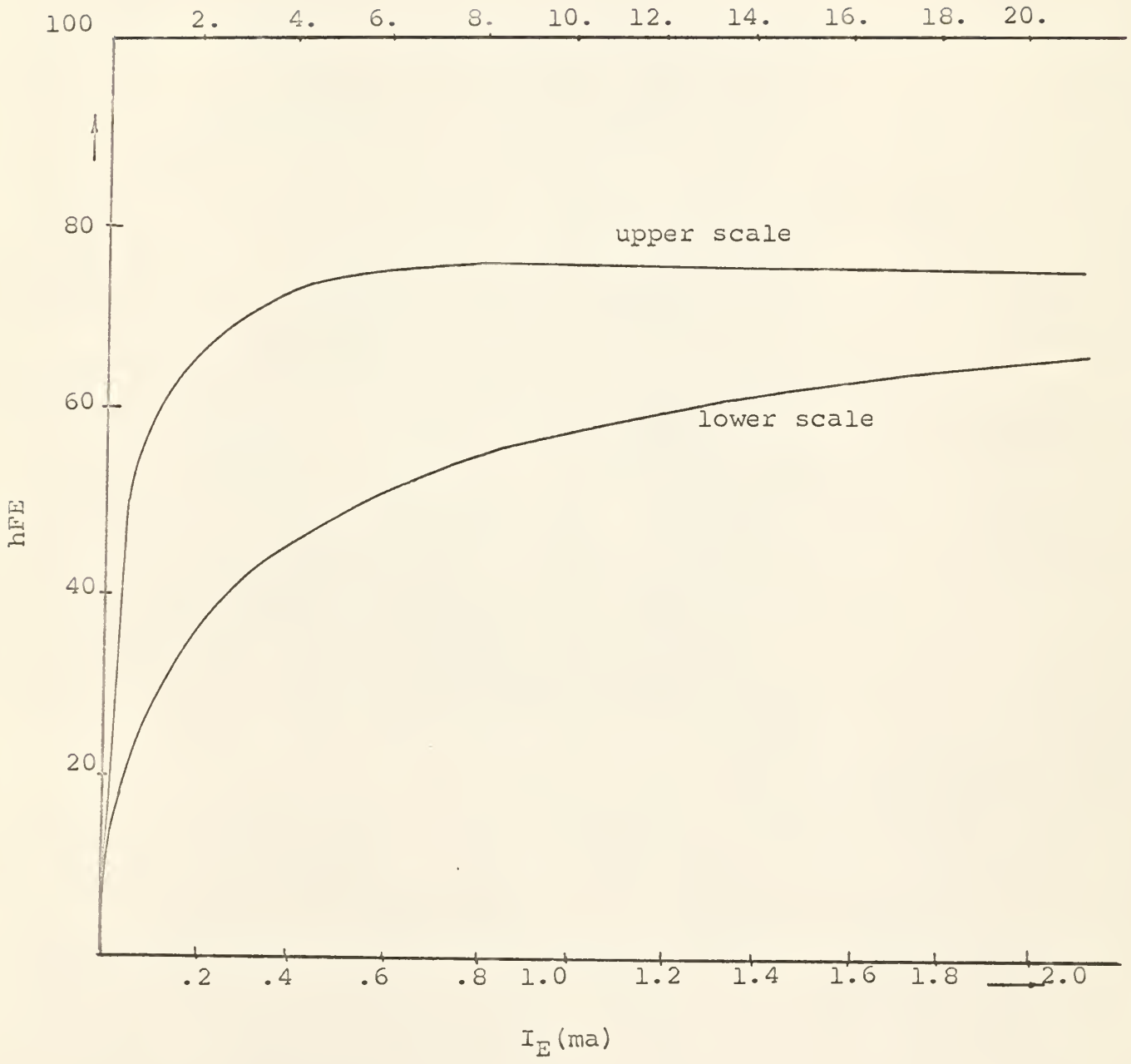

Fig. 16. Common emitter, short circuit current gain versus emitter current.

τ_c is defined as $\tau_c = \frac{\Delta Q_B}{\Delta I_C}$ (55)

By manipulating equations (55) and (54), equation (56) will result.

$$\tau_c = \tau_B \cdot hFE \quad (56)$$

Commonly τ_c is found first and then τ_B is calculated. This is done because the error involved in evaluating τ_c is less than the error in evaluating τ_B.

Base spreading resistance, R_B can be obtained from a small-signal bridge measurement of the $R_B \cdot C_C$ product, Fig. 17.

The values of R_B indicate that R_B is a function of the emitter current and decreases as the emitter current increases; however, these values level off at higher emitter current. For the transistor X, a nominal value of 15 ohms is obtained for the emitter current beyond 3ma. For emitter currents less than 3ma, R_B increases to about twice the nominal value at 1ma.

I_{SC}, μ, C_{C1}, n and hFEI are determined in the same manner as I_{SE}, γ, C_{E1}, and m and hFE respectively, with the exception that the emitter and collector leads are interchanged.

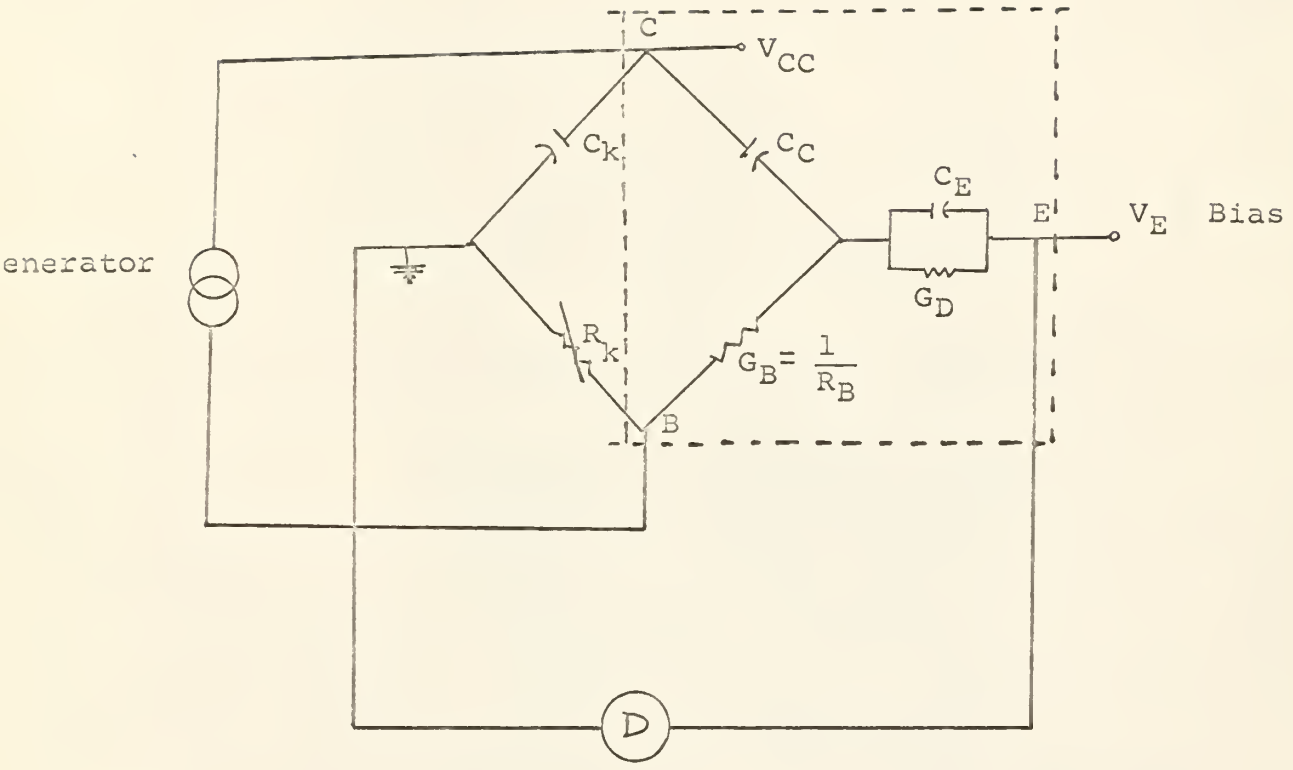

Fig. 17. The diagram used to evaluate R_B.

R_K is Known Resistance.
C_K is Known Capacitance.
D is Detector.

And:

$$R_B = \frac{R_K C_K}{C_C}$$

4. SIMULATION ON THE COMPUTER

The model in Fig. 12 is programmed on IBM 7090. This program can be used on the IBM 709X series. The program is written in the FORTRAN II language. A brief discussion of the program is given below. (See Appendix B)

The time response of the circuit is found by forming node equations and solving for derivatives where there are reactive elements at the node. This yields a system of non-linear differential equations. These equations are:

$$G_B V_B - G_B V_{BP} + (C_{BES} + C_{CBS})\dot{V}_B - C_{CBS}\dot{V}_O = 0 \qquad (59)$$

$$-V_B G_B + (G_B + G_D + G_S)V_{BP} - G_S V_O + (C_E + C_D + C_C + C_S)V_{EP} - (C_C + C_S + C_{CBS})\dot{V}_O = 0 \qquad (60)$$

$$-G_S V_{BP} + G_S V_O - C_{CBS}\dot{V}_B - (C_C + C_S)\dot{V}_{BP} + (C_{CBS} + C_C)\dot{V}_O = -hFEV_{BP}G_D + hFEI\, G_S(V_O - V_{BP}) \qquad (61)$$

Where:

$$V_B = V_{BE} \qquad V_{BP} = V_{B1E} \qquad V_O = V_{CE}$$

$$\dot{V}_B = \frac{dV_B}{dt} \qquad \dot{V}_{BP} = \frac{d}{dt}V_{BP} \qquad \dot{V}_O = \frac{d}{dt}V_O$$

Equations 59 - 61 are solved by a predictor-corrector numerical integration technique. Nonlinear elements are handled by computing their value at each interval of integration step. The

accuracy and running time of this program is highly dependent on the initial value of voltages, the integration interval, and the maximum allowable relative error for each integration interval. The value of 1.0E - 7 has yielded accurate results and is recommended for use. The interval at which the program prints also determines the minimum integration interval which in turn affects the accuracy of the solution. Accurate calculations of the initial condition of the voltages (V_B, V_{BP}, and V_O) will decrease running time and have a solutary effect on the computed response. The input signal to the transistor should not be programmed at the initial time T_O. This is to allow the transients introduced by inconsistent initial conditions to dissipate before applying the input signal.

The functional relationships describing the R_B and hFE as a function of the emitter current are of complex nature; also, these relationships are not very representative of the phenomenom occurring. The values of R_B and hFE as a function of the emitter current are given by the table of values to the computer. An error is introduced in this program to reduce the computing time. This is done by evaluating the present value of R_B and hFE through using the last value of I_E. This error is of no consequence, and the approximation is justifiable, because the variation of the R_B and hFE as a

function of I_E for an integration interval is negligible.

5. MODEL TESTS

The model of Fig. 12 has been exercised in a single saturated inverter circuit, in an emitter follower circuit, and in a three stage d-c coupled amplifier (5). The saturated inverter circuit exhibits the behavior of the model under large signal application. The emitter follower circuit exhibits the behavior of the model under small signal application. The three stage amplifier exhibits behavior of the model under both small and large signal simultaneously. The results indicate that the model is capable of predicting in detail both the steady-state and transient response of the device.

In all three circuits the components were chosen so as not to obscure the device performance. Although planar silicon transistors (Fairchild 1312) were used in the experimental work, the model has more general application. The systems of simultaneous nonlinear differential equations resulting from these circuits have been programmed on the 7090 in conjunction with the described program in part 4 of this paper.

5.1 CIRCUIT CHARACTERIZATION

The circuits used for these studies were carefully constructed to minimize stray inductance and capacitance. The remaining stray capacitances present were measured in the absence of the transistor and added to respective header and land capacitances to form C_{CBS}, C_{EBS}, and C_{CES}. The remaining circuit elements were measured by entirely conventional means. The equivalent resistance of the pulse generator and its termination were added to the lumped resistor in the base lead to form R_G. A carefully calibrated sampling scope driving an X-Y plotter was used to measure the .7 nanosecond ramp input pulse and the output voltage. Shunt capacitance of the scope probes were taken into account where appropriate (5).

5.2 SATURATED INVERTER CIRCUIT

The saturated inverter of Fig. A was driven under the conditions of the resistance R_G with a value of 525 ohms, V_{int} was a pulse with the peak value of 2.5 volts, and the rise time of the .7 nanosecond. Fig. 18 programmed on the 7090 computer as is described. The system of nonlinear differential

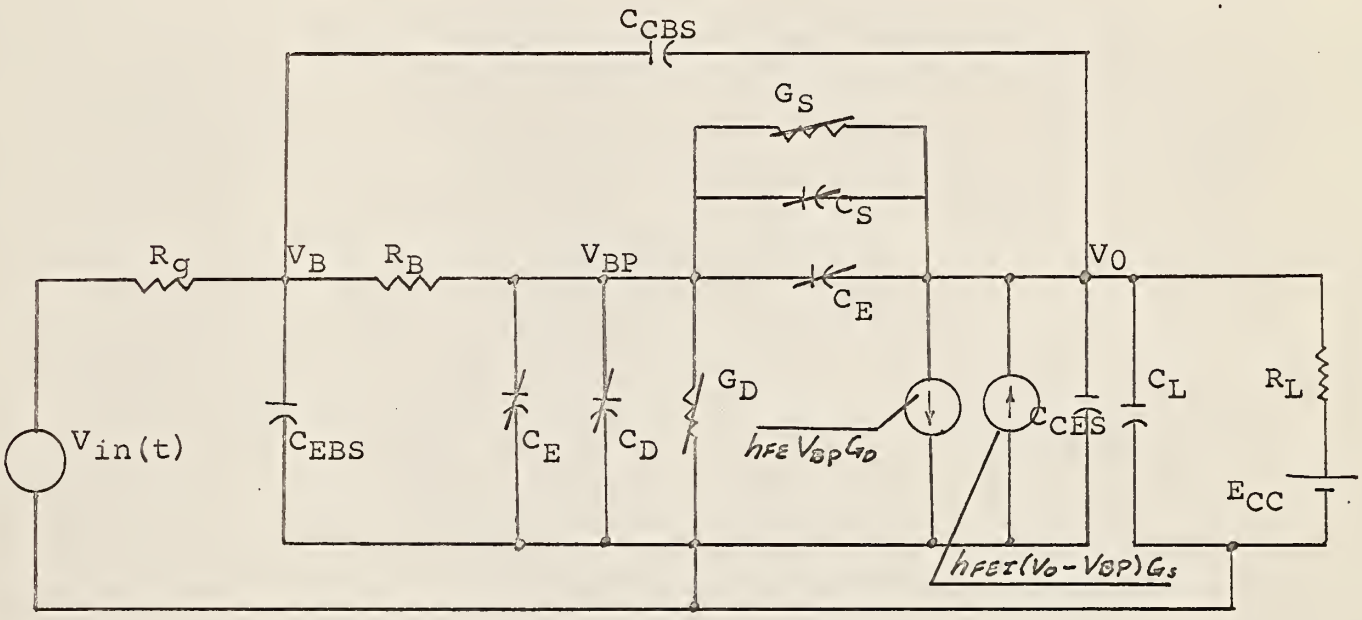

Fig. 18. Nonlinear transistor model in saturating inverter circuit.

$$(G_g + G_B) - G_B V_{BP} + (C_{CBS} + C_{CES})\dot{V}_B - C_{CBS}\dot{V}_0 = G_g V_{in}(t) \tag{62}$$

$$-G_B V_B + (G_B + G_D + G_S)V_{BP} - G_S V_0 + (C_E + C_D + C_C + C_S)\dot{V}_{BP} - (C_S + C_C + C_{CBS})\dot{V}_0 = 0 \tag{63}$$

$$-G_S V_{BP} + (G_L + G_S)V_0 - C_{CBS}\dot{V}_B - (C_C + C_S)\dot{V}_{BP} + (C_{CBS} + C_L + C_C + C_S)\dot{V}_0 = -h_{FE}V_{BP}G_D + E_{CC}G_L + h_{FEI}G_S(V_0 - V_{BP}) \tag{64}$$

equations describing Fig. 18 are given in equations 62 - 64.

The input voltage to the computer was described as shown in Fig. 19 and the functional relationships representing Fig. 19 were given in equations 65 - 71.

$$V_{in} = V_K \qquad 0 \leqslant T < T_0 \qquad (65)$$

$$V_{in} = V_K + V_R(1-e^{-\delta(T-T_0)}) \qquad T_0 \leqslant T < T_R \qquad (66)$$

$$V_{in} = V_L \qquad T_R \leqslant T < T_F \qquad (67)$$

$$V_{in} = V_L + (1-e^{-\alpha(T-T_F)})V_F \qquad T_F \leqslant T < T_Q \qquad (68)$$

$$V_{in} = V_K \qquad T \leqslant T_Q \qquad (69)$$

$$\delta = \frac{-\ln(\frac{V_R - V_L}{V_R - V_K})}{T_R - T_0} \qquad (70)$$

$$\alpha = \frac{\ln(\frac{V_L - V_F}{V_K - V_F})}{T_Q - T_F} \qquad (71)$$

The comparison of experimental and predicted result for saturated inverter Fig. 18 is shown in Fig. 20. The experimental performance of the device agreed with the predicted values better than 10 percent for turn-on delay, turn-on, and turn-off. Only the prediction of storage time did not agree with experimental results. This will be further discussed in section 6 of this paper.

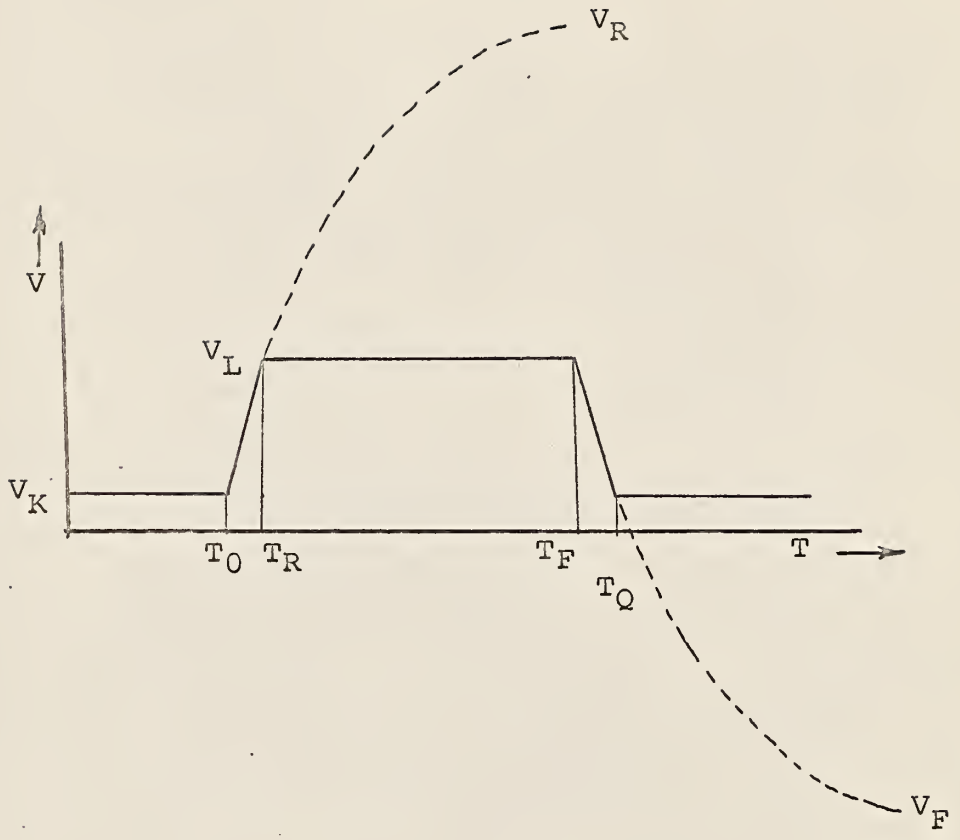

Fig. 19. This form of the input is simulated on the Computer.

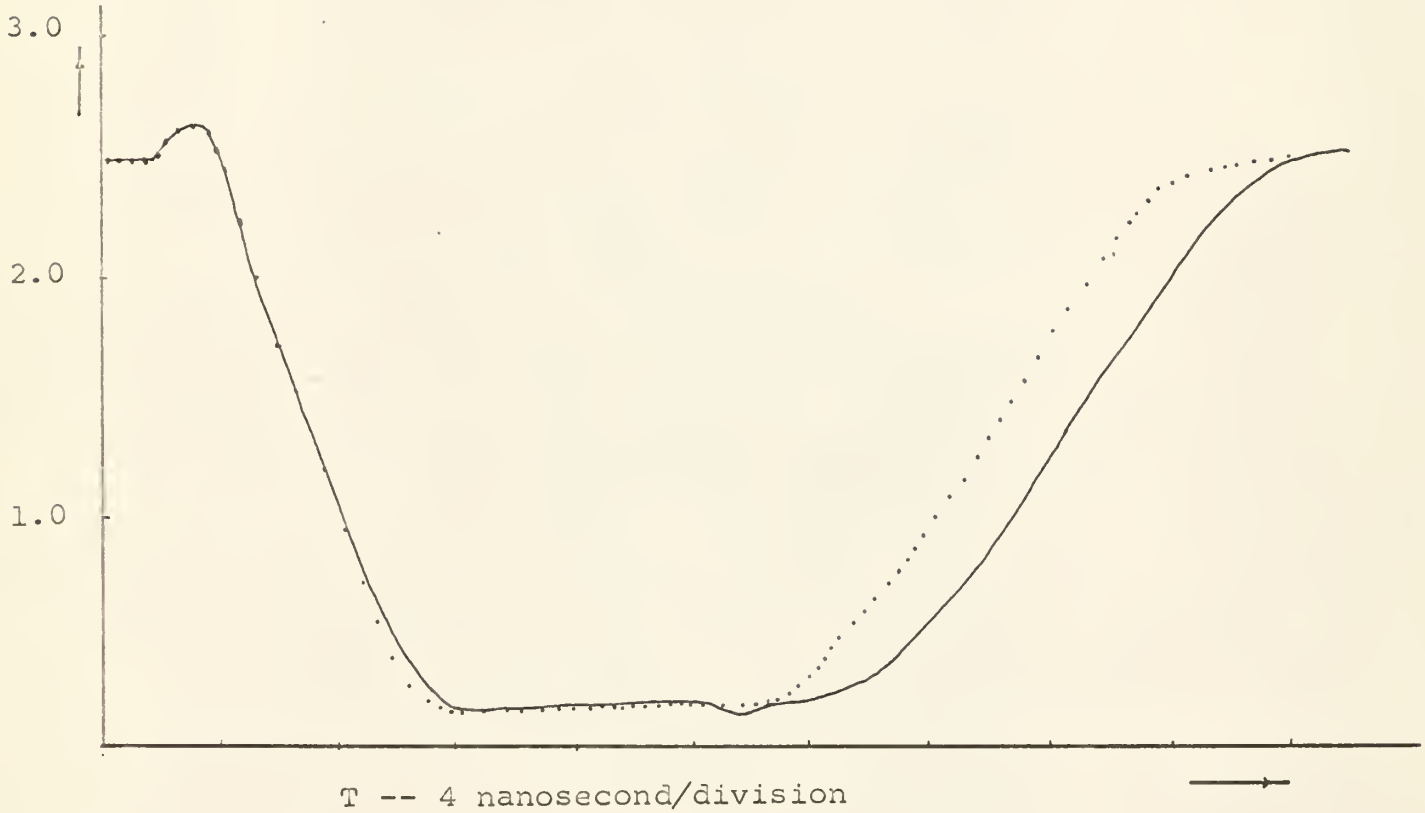

Fig. 20. Comparison of experimental and predicted results for saturated inverter.

Solid line is experimental results.
Dotted line is predicted results.
V_{in} = 2.5 volts with .7 nanosecond rise time.
R_g = 525 ohms.

5.3 EMITTER-FOLLOWER CIRCUIT

The stability of the emitter-follower has been investigated by many authors. It has been pointed out that the input of a transistor in the emitter-follower configuration appears, under certain conditions, to be a capacitance shunted with negative resistance. Therefore, if the driving source to this device appears to be inductive, instability and oscillation are quite likely to occur. Fig. 21 presents an equivalent circuit for a simple emitter-follower. The device model is the same as that used in the saturated inverter circuit with the exception that G_S and C_S were set to zero. The deriving source contains the inductance L necessary for instability. This inductance L in practice is usually caused by lead wire inductance. Fig. 22 shows a comparison of theoretical and experimental results for a representative device (transistor X) and for a value of inductance. The device value used to obtain the emitter-follower results were precisely those used to obtain saturated inverter of Fig. 20. This result demonstrates that this model need not be restricted to large signal applications but is equally useful in representing the device in the "linear" region.

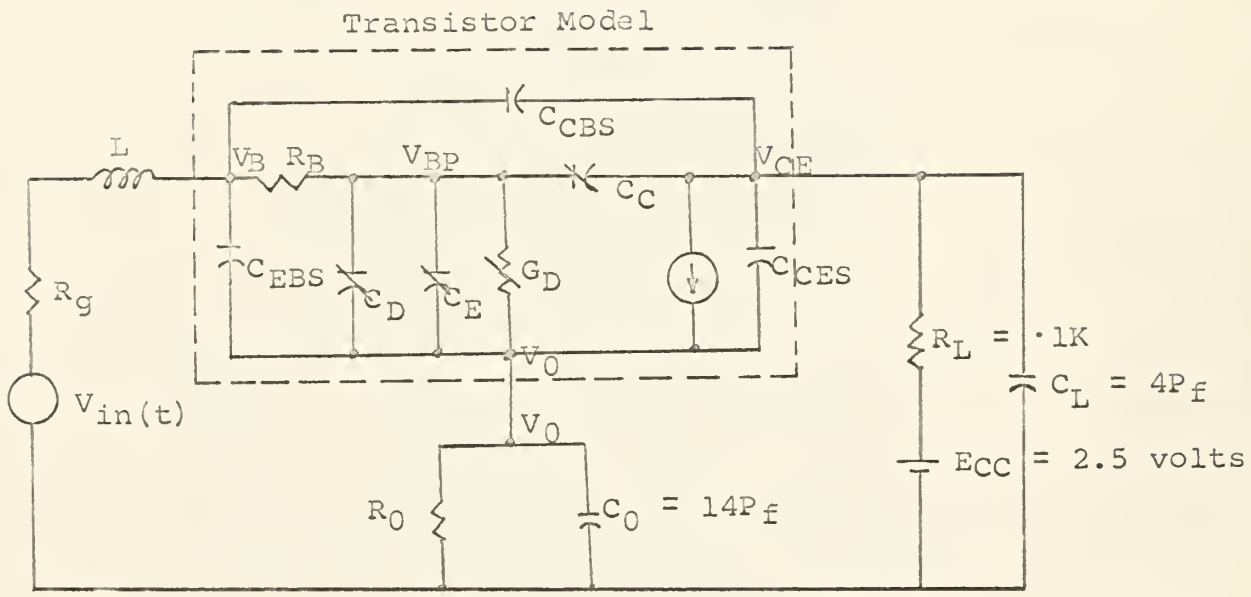

Fig. 21. Nonlinear transistor model in emitter-follower circuit.

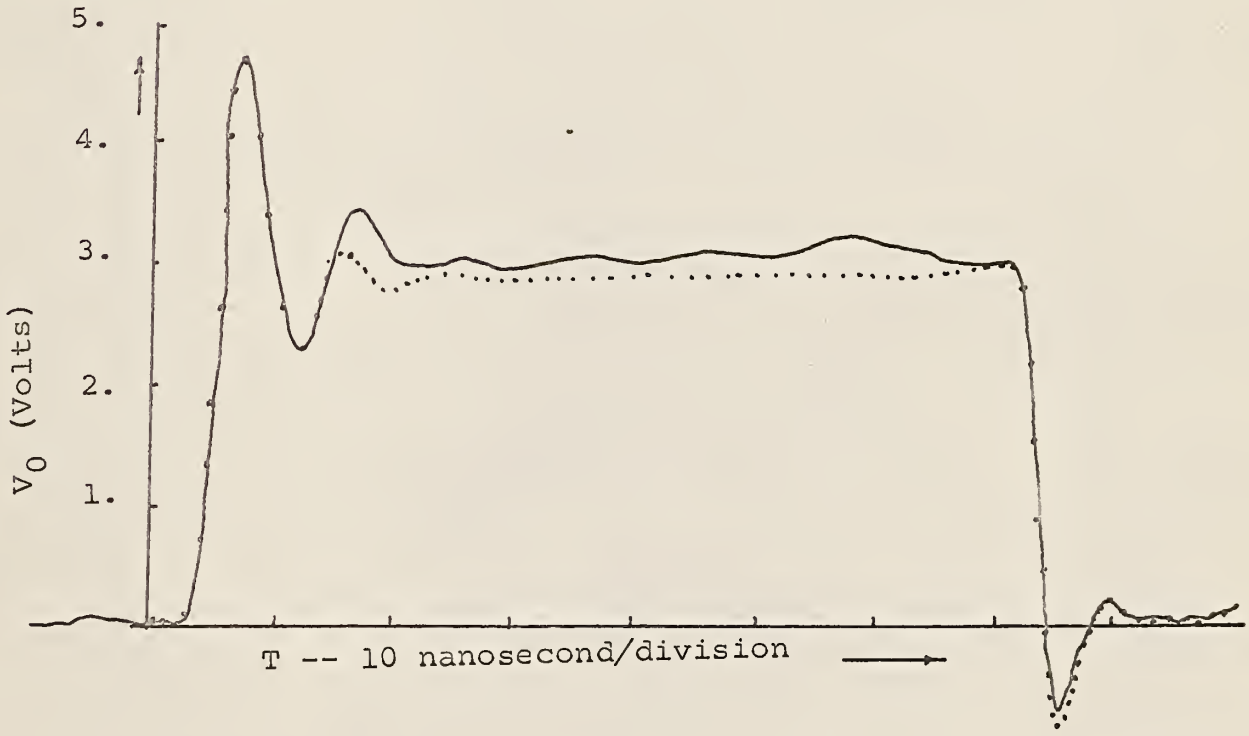

Fig. 22. Comparison of experimental and predicted results for emitter-follower.

$L = 160$ nh
$R_0 = 250$ ohms

$R_g = 50$ ohms.
$V_{in(t)} = 1$ volt

5.4 THREE STAGE D-C COUPLED AMPLIFIER CIRCUIT

The model was exercised further in a three stage d-c coupled amplifier of Fig. 23. The device model was the same as that used in the saturated inverter circuit. The circuit used for this study was carefully constructed to minimize stray inductance. Stray inductances due to the circuit-wire were found to be negligible. No inductance was programmed as it was done for emitter-follower. Fig. 24 shows a comparison of the theoretical and experimental results for a representative device (transistor X). The result indicates that the use of a nonlinear model makes it possible to obtain both the steady-state and transient solution simultaneously.

In the analysis, T_1, T_2 and T_3 are represented by the nonlinear transistor model of Fig. 12.

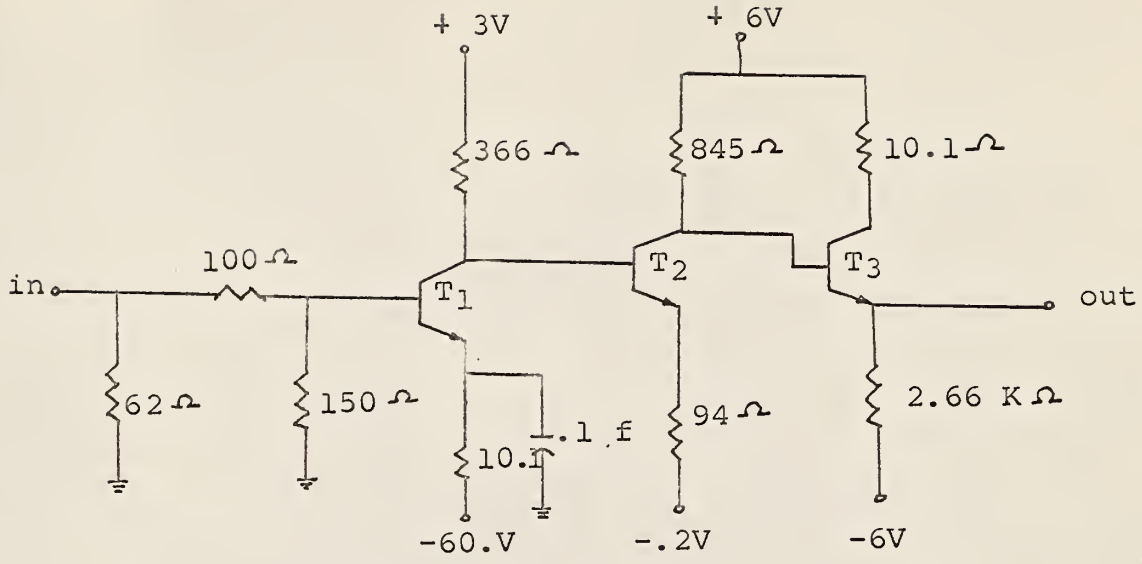

Fig. 23. Three-stage D-C Coupled Amplifier.

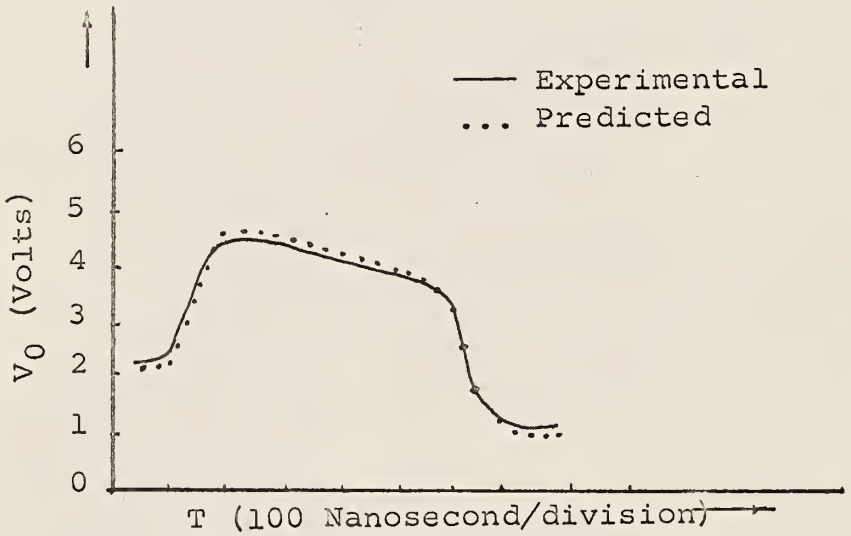

Fig. 24. Comparison of predicted and experimental results for the circuit of Fig. 23.

V_{in} = 5 mV pulse, 500 sec. in duration.

6. MODIFICATION OF THE MODEL

The extrinsic model of Fig. 12 is capable of predicting the turn-on, turn-on delay, turn-off delay, and d-c characteristics of the transistor in detail. However, it fails to predict the turn-off (storage time) in detail. This suggests that the extrinsic model should be further completed. Fig. 25 is a plot of collector deplation capacitance versus junction voltage. The equation (49) is used to describe this phenomena. The result indicates that the equation (49) is only capable of the predicting of the depletion layer capacitance for reversed biased condition. This indicates that the functional relationship used to describe the deplation junction capacitance was inadequate and failed to predict forward biased characteristic. This failure used to be blamed on the 1) difficulty of reproducing the forward biased data characteristic of deplation capacitance, 2) the diffusion capacitance. A careful capacitance measurement with a-c signal as small as 20 microvolts has made it possible to reproduce the forward biased data. The diffusion capacitance values were calculated and they indicated that for emitter junction the calculated value of the diffusion capacitance were very close to the

observed values. However, for collector junction the diffusion capacitance was by order of magnitude smaller than observed value. As a result, a new functional relationship for describing deplation layer capacitance is being adopted. The new functional relationship is capable of predicting depletion layer capacitance for the forward biased condition as well as reversed biased condition within five percent of the measured value. The results are plotted in Fig. 25 and the functional relationship is given by equation (72).

$$C_C = \frac{C_{C1}}{(V_{\phi C} - V_{CB})^m} + \frac{C_{FC1}}{(V_{\phi C} - V_{CB})^p} \qquad (72)$$

Where C_{C1}, m, C_{FC1} and p are found empirically.

Although this new functional relationship is not in exact exponential form, it closely resembles the work done by C. T. Sah and will predict the same result at the limits. C. T. Sah attributes this effect to free carriers in the transistor region (8).

The new functional relationship makes it possible to predict storage time within a few percent. The results are plotted in Fig. 26. The extrinsic model is called complete model when substituting equation (72) for equation (49).

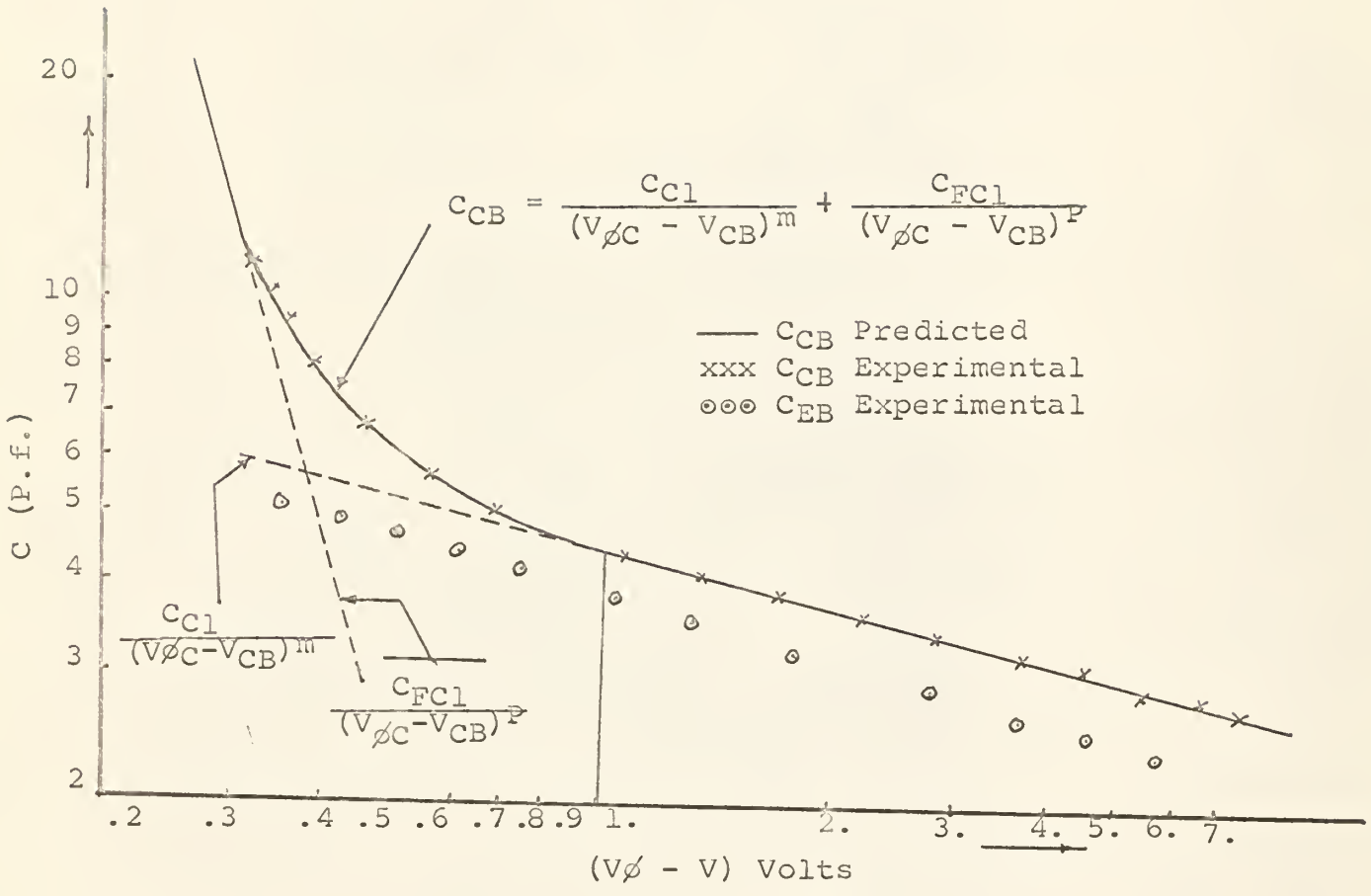

Fig. 25. Collector depletion layer capacitance v.s. voltage across the junction.

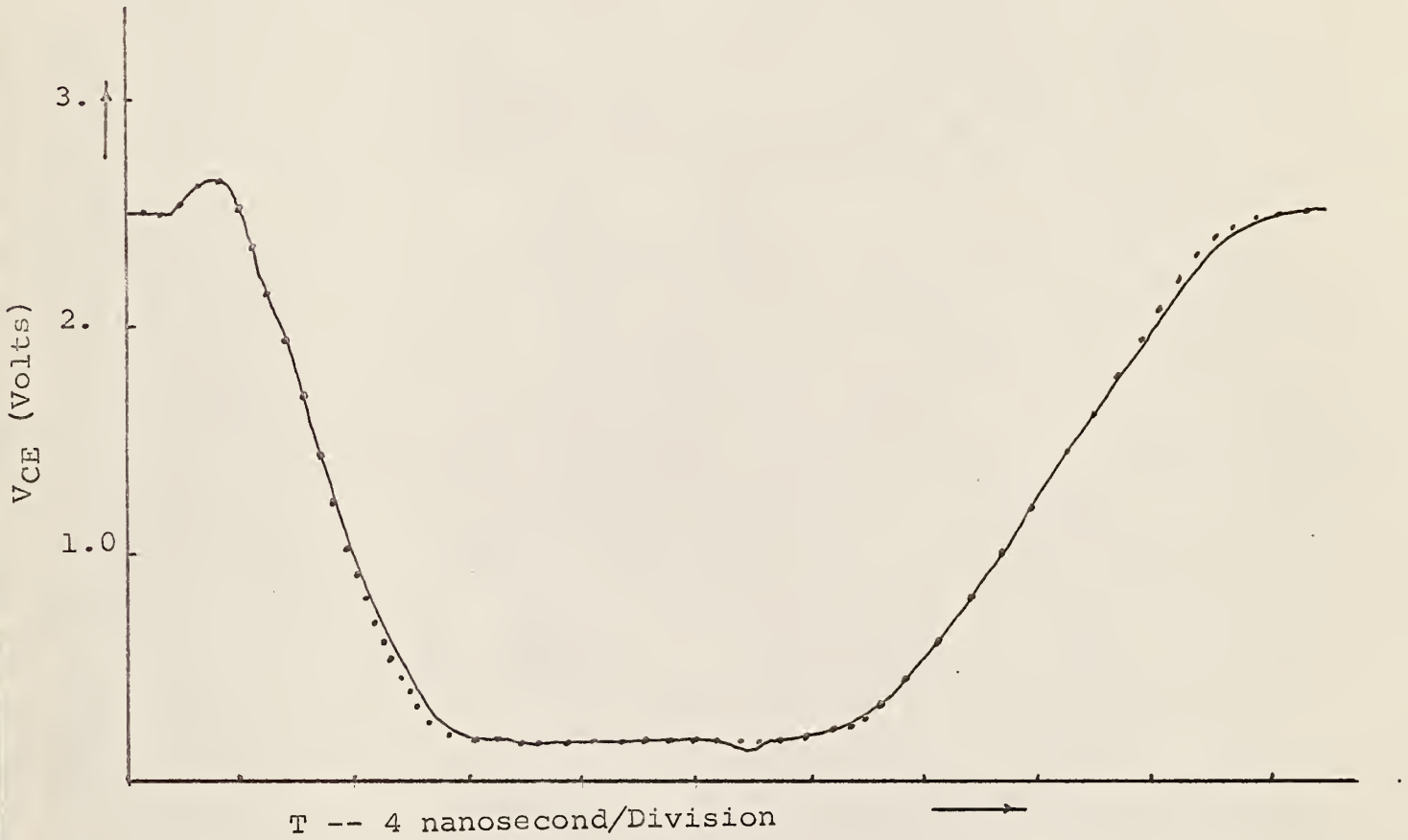

Fig. 26. Comparison of predicted and experimental results for the circuit, Fig. 18.

Solid line = experimental results.
Dotted line = predicted results.

7. SENSITIVITY OF PREDICTED RESULT TO DEVICE AND CIRCUIT PARAMETERS

Every measurement made is subject to a number of errors. In order to determine the influence of measurement errors on the predicted results, nominal values for each parameter were used in the inverter program (5). These results were compared to the results obtained when each nominal value was incremented independently by 5 percent. The sensitivity results indicate that C_C and the parameters that determine base current V_{in}, $R_G + R_B$, and were by far the most important parameters for this circuit. The circuit response is relatively insensitive to parameters such as hFE and τ_b. The results of the sensitivity study make it possible to determine which device parameters need only be specified nominally, thus reducing drastically the number of parameters to be measured.

The program from which these results were obtained has facilities for emitter current dependence of hFE and R_B. However, all the results presented assume constant values for hFE and R_B. The predicted result from nonlinear hFE and R_B agree to the third place with the linear results. If a circuit with a saturation current approaching ma for the transistor X had been chosen, it would be anticipated that results would be a great deal different.

8. CONCLUSION

The results shown in this paper demonstrate the feasibility of using a nonlinear, equivalent circuit model to represent a transistor in large signal, small signal and both large signal and small signal operation simultaneously. Although the range of devices and circuit conditions is quite limited in this study, it is significant to note that none of the devices strayed more than ten percent from their predicted behavior, and the majority of this is attributed to the great dependence the circuit has to $V_{in(t)}$.

The model does not require any advanced programming and machine running time is not lengthy. Machine running time for the results of saturated inverter circuit was forty seconds, including read and write tape.

The model does an excellent job in predicting transient time. The model is not a cumbersome model. It does not introduce any new circuit elements. It is compatible with the other circuit elements to which it is to be connected and it does not require a circuit designer to be accustomed to new circuit elements. The relationship to device physics is relatively clear, and the model is capable of providing device people with information about their products.

The linear form of the model has found wide acceptance in the design of small signal amplifiers. The introduction of nonlinear elements intensifies the value of this model for small signal design since it permits simultaneous a-c and d-c analysis.

Parameters of the model can be evaluated easily with conventional techniques. Circuit elements and device parameters may be optomized long before the devices are available. This approach is particularly useful in the design of integrated circuit where the trimming of a circuit is impractical. The model can be used as the basis of an integrated specification which would include large signal and small signal application.

The model and the paragram can be combined to a subroutine paragram. The subroutine can be used instead of transistor in the circuit, and the performance of the circuit can be predicted easily.

In short, this model is a practical model.

ACKNOWLEDGMENTS

The author wishes to express his deep appreciation to Mr. Joseph E. Ward, Jr., of the Department of Electrical Engineering for his guidance and encouragement during the preparation of this paper.

The author also wishes to express his gratitude to R. J. Wilfinger of the International Business Machine Corporation, who contributed to the work on this study, and to the staff of the Department of Electrical Engineering of Kansas State University for their useful discussion during the preparation of this paper.

REFERENCES

1. Ebers, J. J. and J. L. Moll.
Large-signal Behavior of Junction Transistors. Proc. IRE, December, 1954, pp. 1761-1772.

2. Ghausi, M. S.
Principles and Design of Linear Active Circuits. New York: McGraw-Hill, 1965, Chapters 6, 7, 8 and 9.

3. Giacoletto, L. J.
Study of PNP Alloy Junction Transistors from D-C through Medium Frequencies. RCA Review, December, 1954, pp. 506-562.

4. Gray, P. E., D. DeWitt, A. R. Boothroyd and J. F. Gibbons.
Physical Electronics and Circuit Models of Transistors. New York: John Wiley & Sons, Inc., 1964, Chapter 9.

5. Kiankhooy-Fard, P. and R. J. Wilfinger.
A Nonlinear Transistor Model for the Prediction of Circuit Transient Response. 1964 International Solid-State Circuits Conference, p. 46.

6. Moll, J. L.
Large-Signal Transient Response of Junction Transistors. Proc. IRE, December, 1954, pp. 1773-1784.

7. Nanavatti, R. P.
An Introduction to Semiconductor Electronics. New York: McGraw-Hill, 1963, Chapters 9 and 10.

8. Sah, C. T.
Effects of Electrons and Holes on the Transition Layer Characteristics of Linearly Graded P-N Junctions. Proc. IRE, March, 1961.

APPENDIX A

Transistor X is a NPN planar silicon transistor manufactured by Fairchild and was designated type 2B8.

The breakdown voltage of either junction is about 9 volts. The hFE of the transistor is about 75, the detail hFE characteristic is given in Fig. 16 of this paper. Other characteristics of this transistor are given in the device characteristics of this paper.

Other types of transistors were used in the experimental work, which all have exhibited similar results as transistor X. However, all the data and results represented in this paper are of transistor X.

APPENDIX B

The listing of the program used to predict the theoretical value is given in this Appendix. The data and programming of this Appendix is a portion of a published paper by the International Business Machines Corporation which is a supplement to reference (X). The paper identification is as follows.

Identification

Nonlinear Transistor model for the prediction of circuit transient response

R. J. Wilfinger/P. Kiankhooy-Fard/S. C. Plumb

Program Description - A. Selby, Scientific Computation, International Business Machines Corporation, Components Division, Fishkill, New York

```
C     TRANSIST V            CF ADDITION
C
C     VERSION WITH HYPERBOLIC FORM OF CF
C
      DIMENSION A(80), AIR(50), AIH(50), RB(50), HFE(50), V(4), VP(4),
     $ VC(4), TBL(16)
      EQUIVALENCE (V(1), VBP), (V(2), VO), (V(3), VB), (VP(1), DVBP),
     $  (VP(2), DVO), (VP(3), DVB), (V(4), VG), (DVG, VP(4))
      READ INPUT TAPE 2, 5, A
 5    FORMAT (20A4)
 1    READ INPUT TAPE 2, 2, IVSN, ERR
 2    FORMAT (I5, 5X, E5.0)
      READ INPUT TAPE 2, 3, VG,VB,VBP,VO,DT,TMAX
      READ INPUT TAPE 2, 3, VK, VL, VR, T0, TR
      READ INPUT TAPE 2, 3, VF, TF, TQ
      READ INPUT TAPE 2, 3, RG, CBES, CCBS, RL, CL, ECC
      READ INPUT TAPE 2, 3,  CCES,R2,C2,R3,R,C
      READ INPUT TAPE 2, 3, AISE, GAM, Q, P, TB, VPHI
      READ INPUT TAPE 2, 3, CE1, EM, CC1, EN,AA , BB
      READ INPUT TAPE 2, 3,AISC , AMU , VPHC, TS, HFEI ,HFX
 3    FORMAT (6E12.4)
      READ INPUT TAPE 2, 4, N, (AIH(I), HFE(I), I = 1,N)
      READ INPUT TAPE 2, 4, M, (AIR(I), RB(I), I = 1,M)
 4    FORMAT (I5/ (2E12.4))
      CALL GIRL
      CALL TITLE
      WRITE OUTPUT TAPE 3, 6, A(1), VB, A(2), VBP, A(3), VO, A(4), DT,
     $A(5), TMAX
      WRITE OUTPUT TAPE 3, 6, A(6), VK, A(7), VL, A(8), VR, A(9), T0, A(
     $10), TR
      WRITE OUTPUT TAPE 3, 6, A(11), VF, A(12), TF, A(13), TQ,A(55),CCES
      WRITE OUTPUT TAPE 3, 6, A(14), RG, A(15), CBES, A(16), CCBS, A(17)
     $, RL, A(18), CL, A(19), ECC
      WRITE OUTPUT TAPE 3, 6, A(20), AISE, A(21), GAM, A(22), Q, A(23),
     $ P, A(24), AISC, A(25), AMU
      WRITE OUTPUT TAPE 3, 6, A(26), VPHI, A(27), CE1, A(28), EM, A(29),
     $ CC1, A(30), EN, A(31), HFEI
      WRITE OUTPUT TAPE 3, 6, A(53), VG, A(56), R, A(57), C, A(58), R2,
     $ A(59), C2, A(60), R3
      GG = 1./RG
      GL = 1./RL
      G = 1./R
      G2 = 1./R2
      G3 = 1./R3
      ALPHA = LOGF((VL - VF)/(VK - VF))/(TQ - TF)
      DELTA = -LOGF((VR - VL)/(VR - VK))/(TR - T0)
      WRITE OUTPUT TAPE 3, 6, A(32), TS, A(33), TB, A(51), ALPHA, A(52),
     $ DELTA, A(61), AA, A(62), BB
      WRITE OUTPUT TAPE 3, 6, A(64),VPHC
 6    FORMAT (1X, 6(A4, E12.5, 4X))
      T = 0.
      TC =0.
      I = 0
      NN = 4
```

```
      DO [illegible] I [illegible]
      [illegible] = V[illegible]
 [illegible]  IF (T - TC) [illegible]
 2[illegible]  V[illegible] = VX
      GO TO 100
 [illegible]  IF (T - TR) [illegible]
      VI[illegible] = V[illegible] [illegible] (T - T[illegible])
      GO TO 100
 [illegible]  IF (T - TF) [illegible]
 [illegible]  [illegible] = V[illegible]
      GO TO 100
 [illegible]  IF (T - TC[illegible]) [illegible]
 [illegible]  VIN = VF + [illegible] - [illegible]PF [illegible]-ALPHA*(T - TF))
 10[illegible]  IF (T) 1[illegible] 10
 1[illegible]0  A[illegible] = [illegible] D[illegible]F*CB + (VO - ECC)*GL + DVO*CL +GG*(VB - VIN)
      IF (AIE - A[illegible](1)) [illegible]120,130
 120  HFX = HFE(1
      GO TO 160
 130  DO 140 I = 2,[illegible]
      IF (AIE - AIH(I)) 1[illegible],150 140
 140  CONTINUE
      HFX = HFE(N)
      GO TO 160
 150  HFX = HFE(I-1) + (AIE - AIH(I-1))/(AIH(I) - AIH(I-1))*(HFE(I) -
     $ HFE(I-1))
 160  GO TO 165
 165  IF (AIE - AIR(1)) 170,170,180
 170  RBX = RB(1
      GO TO 210
 180  DO 190 I = 2,[illegible]
      IF (AIE - AIR(I)) 2[illegible],200,190
 190  CONTINUE
      RBX = RB(M)
      GO TO 210
 200  RBX = RB(I-1) + (AIE - AIR(I-1))/(AIR(I) - AIR(I-1))*(RB(I) - RB(I
     $ - 1))
 210  X = EXPF(CA[illegible]*VBP)
      Y = EXPF([illegible](VBP - VO))
 215  GD =(AISE*(X-1.))/((HFX+1.)*VBP)
      CD=(T[illegible]GAM[illegible]SE*X)/(HFX+1.)
      CE = CE1/(VPHI - VBP)**EN
      CF = AA/(VPHI - (VBP - VO))**BB
      CC = CC1/(VO - VBP + VPHC)**EN
      GS=( AISC*(Y-1.))/( HFEI+ 1.)*(VBP -VO))
      CS= (TS [illegible] (AISC [illegible] Y))/( HFEI +1.)  +CF
      GB = 1./RBX
      [illegible]A = (VB - VBP) GD + VB*C2 + (VG - VIN)*GG
      [illegible] = VBP*(GB + GD + GS) - VB*GB - VO*GS
      X[illegible] = VO*(GL + GS) - VBP*GS + HFX*VBP*GD - ECC*GL - HFEI*GS*(VBP -
     $ VO)) + VO*G3
      XD = CRES + CCBG + C2
      [illegible] = CCB[illegible]
      XG = CE + CD + CC + CS
      [illegible] = CC + CS
      XJ = CCBS + CL + CC + C[illegible] + CC[illegible]
      DVO = -([illegible]*(XC - [illegible]I/XG) + [illegible]XE)/(-[illegible]E**2 + XD*(-XI**2/XG + XJ))
```

```
T 0.24000E 01   V8P 0.26360E-00 DVP 0.43404E-00  VC 0.25924E 01 DVO 0.10332E-00  V8 0.31483E-00 DV8 0.42496E-00 VIN 0.25000E 01
                IE-0.82963E-01 HFE 0.85000E 02  RB 0.15000E-01  GD 0.11046E-07  GS 0.32610E-07  CO 0.85477E-06  CE 0.52911E 01
                CC 0.33835E 01  CS 0.82064E-04  VG 0.31483E-00 DVG 0.42496E-00  CF 0.82064E-04

T 0.26000E 01   V8P 0.34646E-00 DVP 0.39556E-00  VC 0.26093E 01 DVO 0.67966E-01  V8 0.39597E-00 DV8 0.38741E-00 VIN 0.25000E 01
                IE-0.36119E-01 HFE 0.85000E 02  RB 0.15000E-01  GD 0.16050E-06  GS 0.33560E-07  CO 0.16325E-04  CE 0.55272E 01
                CC 0.34016E 01  CS 0.90796E-04  VG 0.39597E-00 DVG 0.38741E-00  CF 0.90796E-04

T 0.28000E 01   V8P 0.42218E-00 DVP 0.36241E-00  VC 0.26202E 01 DVO 0.41635E-01  V8 0.47015E-00 DV8 0.35512E-00 VIN 0.25000E 01
                IE-0.17186E-01 HFE 0.85000E 02  RB 0.15000E-01  GD 0.19484E-05  GS 0.34550E-07  CO 0.24148E-03  CE 0.57961E 01
                CC 0.34198E 01  CS 0.10052E-03  VG 0.47015E-00 DVG 0.35512E-00  CF 0.10052E-03

T 0.30000E 01   V8P 0.49168E-00 DVP 0.33290E-00  VC 0.26264E 01 DVO 0.21799E-01  V8 0.53826E 00 DV8 0.32674E-00 VIN 0.25000E 01
                IE-0.43205E-02 HFE 0.85000E 02  RB 0.15000E-01  GD 0.19827E-04  GS 0.35574E-07  CO 0.28618E-02  CE 0.61106E 01
                CC 0.34381E 01  CS 0.11123E-03  VG 0.53826E 00 DVG 0.32674E-00  CF 0.11123E-03

T 0.32000E 01   V8P 0.55548E 00 DVP 0.30457E-00  VC 0.26291E 01 DVO 0.58698E-02  V8 0.60087E 00 DV8 0.30278E-00 VIN 0.25000E 01
                IE-0.48983E-02 HFE 0.85000E 02  RB 0.15000E-01  GD 0.17002E-03  GS 0.36622E-07  CO 0.27725E-01  CE 0.64905E 01
                CC 0.34562E 01  CS 0.12292E-03  VG 0.60087E 00 DVG 0.30278E-00  CF 0.12292E-03

T 0.34000E 01   V8P 0.61346E 00 DVP 0.27244E-00  VC 0.26285E 01 DVO-0.13823E-01  V8 0.65784E 00 DV8 0.27153E-00 VIN 0.25000E 01
                IE-0.77463E-01 HFE 0.85000E 02  RB 0.15000E-01  GD 0.12119E-02  GS 0.37687E-07  CO 0.21826E-00  CE 0.69640E 01
                CC 0.34741E 01  CS 0.13556E-03  VG 0.65784E 00 DVG 0.27153E-00  CF 0.13556E-03

T 0.36000E 01   V8P 0.66313E 00 DVP 0.21826E-00  VC 0.26216E 01 DVO-0.63761E-01  V8 0.70691E 00 DV8 0.21832E-00 VIN 0.25000E 01
                IE-0.54089E 00 HFE 0.85000E 02  RB 0.15000E-01  GD 0.65546E-02  GS 0.38776E-07  CO 0.12759E 01  CE 0.75475E 01
                CC 0.34918E 01  CS 0.14929E-03  VG 0.70691E 00 DVG 0.21832E-00  CF 0.14929E-03

T 0.38000E 01   V8P 0.69896E 00 DVP 0.13886E-00  VC 0.25984E 01 DVO-0.17751E-00  V8 0.74241E 00 DV8 0.13674E-00 VIN 0.25000E 01
                IE-0.16551E 01 HFE 0.85000E 02  RB 0.15000E-01  GD 0.22315E-01  GS 0.39978E-07  CO 0.45792E 01  CE 0.81692E 01
                CC 0.35107E 01  CS 0.16540E-03  VG 0.74241E 00 DVG 0.13674E-00  CF 0.16540E-03

T 0.40000E 01   V8P 0.72017E 00 DVP 0.78306E-01  VC 0.25493E 01 DVO-0.31035E-00  V8 0.76293E 00 DV8 0.75098E-01 VIN 0.25000E 01
                IE-0.31886E 01 HFE 0.85000E 02  RB 0.15000E-01  GD 0.45986E-01  GS 0.41514E-07  CO 0.97222E 01  CE 0.86846E 01
                CC 0.35339E 01  CS 0.18748E-03  VG 0.76293E 00 DVG 0.75098E-01  CF 0.18748E-03

T 0.42000E 01   V8P 0.73234E 00 DVP 0.46483E-01  VC 0.24768E 01 DVO-0.40702E-00  V8 0.77428E 00 DV8 0.47951E-01 VIN 0.25000E 01
                IE-0.46176E 01 HFE 0.85000E 02  RB 0.15000E-01  GD 0.69654E-01  GS 0.43530E-07  CO 0.14974E 02  CE 0.90655E 01
                CC 0.35629E 01  CS 0.21903E-03  VG 0.77428E 00 DVG 0.47951E-01  CF 0.21903E-03

T 0.44000E 01   V8P 0.73999E 00 DVP 0.31358E-01  VC 0.23893E 01 DVO-0.46221E-00  V8 0.78130E 00 DV8 0.30079E-01 VIN 0.25000E 01
                IE-0.58924E 01 HFE 0.85000E 02  RB 0.15000E-01  GD 0.90387E-01  GS 0.46043E-07  CO 0.19633E 02  CE 0.93515E 01
                CC 0.35971E 01  CS 0.26254E-03  VG 0.78130E 00 DVG 0.30079E-01  CF 0.26254E-03

T 0.46000E 01   V8P 0.74539E 00 DVP 0.23186E-01  VC 0.22937E 01 DVO-0.48974E-00  V8 0.78637E 00 DV8 0.27300E-01 VIN 0.25000E 01
                IE-0.70269E 01 HFE 0.85000E 02  RB 0.15000E-01  GD 0.10879E-00  GS 0.49046E-07  CO 0.23803E 02  CE 0.95842E 01
                CC 0.36351E 01  CS 0.32066E-03  VG 0.78637E 00 DVG 0.27300E-01  CF 0.32066E-03

T 0.48000E 01   V8P 0.74959E 00 DVP 0.18915E-01  VC 0.21944E 01 DVO-0.50176E 00  V8 0.79037E 00 DV8 0.19239E-01 VIN 0.25000E 01
                IE-0.81145E 01 HFE 0.85000E 02  RB 0.15000E-01  GD 0.12556E-00  GS 0.52562E-07  CO 0.27620E 02  CE 0.97851E 01
                CC 0.36764E 01  CS 0.39728E-03  VG 0.79037E 00 DVG 0.19239E-01  CF 0.39728E-03

T 0.50000E 01   V8P 0.75308E 00 DVP 0.15941E-01  VC 0.20935E 01 DVO-0.50555E 00  V8 0.79379E 00 DV8 0.19988E-01 VIN 0.25000E 01
                IE-0.91611E 01 HFE 0.85000E 02  RB 0.15000E-01  GD 0.14151E-00  GS 0.56654E-07  CO 0.31282E 02  CE 0.99695E 01
                CC 0.37204E 01  CS 0.49808E-03  VG 0.79379E 00 DVG 0.19988E-01  CF 0.49808E-03

T 0.52000E 01   V8P 0.75609E 00 DVP 0.13610E-01  VC 0.19923E 01 DVO-0.50469E 00  V8 0.79685E 00 DV8 0.28337E-01 VIN 0.25000E 01
                IE-0.10196E 02 HFE 0.85000E 02  RB 0.15000E-01  GD 0.15693E-00  GS 0.61430E-07  CO 0.34830E 02  CE 0.10143E 02
                CC 0.37671E 01  CS 0.63133E-03  VG 0.79685E 00 DVG 0.28337E-01  CF 0.63133E-03

T 0.54000E 01   V8P 0.75875E 00 DVP 0.12509E-01  VC 0.18915E 01 DVO-0.50281E 00  V8 0.79944E 00 DV8 0.15563E-01 VIN 0.25000E 01
                IE-0.11196E 02 HFE 0.85000E 02  RB 0.15000E-01  GD 0.17187E-00  GS 0.67043E-07  CO 0.38279E 02  CE 0.10309E 02
                CC 0.38165E 01  CS 0.80887E-03  VG 0.79944E 00 DVG 0.15563E-01  CF 0.80887E-03

T 0.56000E 01   V8P 0.76115E 00 DVP 0.11110E-01  VC 0.17913E 01 DVO-0.49866E-00  V8 0.80190E 00 DV8 0.20984E-01 VIN 0.25000E 01
                IE-0.12197E 02 HFE 0.85000E 02  RB 0.15000E-01  GD 0.18661E-00  GS 0.73724E-07  CO 0.41693E 02  CE 0.10471E 02
```

```
T 0.90000E 01   VBP 0.78246E 00 DVP 0.16464E-02 VC 0.32582E-00 CVC-0.26214E-00 VB 0.82616E 00 OVB 0.63605E-02 VIN 0.25000E 01
                IE-0.25967E 02 HFE 0.85000E 02 RB 0.15000E-01 GD 0.38737E-00 GS 0.29826E-01 ID 0.88572E 02 CE 0.12876E 02
                CC 0.58787E 01  CS 0.33293E 01 VG 0.82616E 00 CVG 0.63605E-02 CF 0.29685E 01

T 0.92000E 01   VBP 0.78269E 00 DVP 0.67757E-03 VC 0.28021E-00 CVC-0.19366E-00 VB 0.82740E 00 OVB 0.57500E-02 VIN 0.25000E 01
                IE-0.26160E 02 HFE 0.85000E 02 RB 0.15000E-01 GD 0.39039E-00 GS 0.91278E-01 ID 0.89690E 02 CE 0.12920E 02
                CC 0.60932E 01  CS 0.70782E 01 VG 0.82740E 00 CVG 0.57500E-02 CF 0.58632E 01

T 0.94000E 01   VBP 0.78277E 00 DVP 0.22492E-03 VC 0.24769E-00 CVC-0.13445E-00 VB 0.82839E 00 OVB 0.40953E-02 VIN 0.25000E 01
                IE-0.26250E 02 HFE 0.85000E 02 RB 0.15000E-01 GD 0.39147E-00 GS 0.20325E-00 ID 0.89149E 02 CE 0.12935E 02
                CC 0.62725E 01  CS 0.13055E 02 VG 0.82839E 00 CVG 0.40953E-02 CF 0.10174E 02

T 0.96000E 01   VBP 0.78280E 00 DVP 0.15387E-03 VC 0.22513E-00 CVC-0.94097E-01 VB 0.82905E 00 OVB 0.26429E-02 VIN 0.25000E 01
                IE-0.26311E 02 HFE 0.85000E 02 RB 0.15000E-01 GD 0.39193E-00 GS 0.35476E-00 ID 0.90059E 02 CE 0.12942E 02
                CC 0.64138E 01  CS 0.20777E 02 VG 0.82905E 00 CVG 0.26429E-02 CF 0.15536E 02

T 0.98000E 01   VBP 0.78284E 00 DVP 0.18199E-03 VC 0.20906E-00 CVC-0.68518E-01 VB 0.82948E 00 OVB 0.17565E-02 VIN 0.25000E 01
                IE-0.26372E 02 HFE 0.85000E 02 RB 0.15000E-01 GD 0.39238E-00 GS 0.52854E 00 ID 0.90165E 02 CE 0.12949E 02
                CC 0.65252E 01  CS 0.29583E 02 VG 0.82948E 00 CVG 0.17565E-02 CF 0.21549E 02

T 1.00000E 01   VBP 0.78288E 00 DVP 0.20102E-03 VC 0.19711E-00 CVC-0.52083E-01 VB 0.82978E 00 OVB 0.12452E-02 VIN 0.25000E 01
                IE-0.26422E 02 HFE 0.85000E 02 RB 0.15000E-01 GD 0.39290E-00 GS 0.71112E 00 ID 0.90289E 02 CE 0.12956E 02
                CC 0.66146E 01  CS 0.38941E 02 VG 0.82978E 00 CVG 0.12452E-02 CF 0.27906E 02

T 0.10200E 02   VBP 0.78292E 00 DVP 0.20055E-03 VC 0.18786E-00 CVC-0.41013E-01 VB 0.82999E 00 OVB 0.94738E-03 VIN 0.25000E 01
                IE-0.26468E 02 HFE 0.85000E 02 RB 0.15000E-01 GD 0.39345E-00 GS 0.89511E 00 ID 0.90415E 02 CE 0.12964E 02
                CC 0.66882E 01  CS 0.48550E 02 VG 0.82999E 00 CVG 0.94738E-03 CF 0.34440E 02

T 0.10400E 02   VBP 0.78296E 00 DVP 0.18887E-03 VC 0.18048E-00 CVC-0.33211E-01 VB 0.83015E 00 OVB 0.78815E-03 VIN 0.25000E 01
                IE-0.26509E 02 HFE 0.85000E 02 RB 0.15000E-01 GD 0.39398E-00 GS 0.10761E 01 ID 0.90546E 02 CE 0.12972E 02
                CC 0.67502E 01  CS 0.58205E 02 VG 0.83015E 00 CVG 0.78815E-03 CF 0.41031E 02

T 0.10600E 02   VBP 0.78299E 00 DVP 0.17216E-03 VC 0.17443E-00 CVC-0.27492E-01 VB 0.83027E 00 OVB 0.75109E-03 VIN 0.25000E 01
                IE-0.26546E 02 HFE 0.85000E 02 RB 0.15000E-01 GD 0.39447E-00 GS 0.12514E 01 ID 0.90663E 02 CE 0.12979E 02
                CC 0.68031E 01  CS 0.67772E 02 VG 0.83027E 00 CVG 0.75109E-03 CF 0.47598E 02

T 0.10800E 02   VBP 0.78302E 00 DVP 0.78962E-04 VC 0.16939E-00 CVC-0.23171E-01 VB 0.83050E 00 OVB 0.69949E-02 VIN 0.25000E 01
                IE-0.26583E 02 HFE 0.85000E 02 RB 0.15000E-01 GD 0.39495E-00 GS 0.14205E 01 ID 0.90778E 02 CE 0.12986E 02
                CC 0.68492E 01  CS 0.77202E 02 VG 0.83050E 00 CVG 0.69949E-02 CF 0.54110E 02

T 0.11000E 02   VBP 0.78306E 00 DVP 0.13233E-03 VC 0.16510E-00 CVC-0.19799E-01 VB 0.83046E 00 OVB 0.12798E-02 VIN 0.25000E 01
                IE-0.26608E 02 HFE 0.85000E 02 RB 0.15000E-01 GD 0.39533E-00 GS 0.15805E 01 ID 0.90869E 02 CE 0.12992E 02
                CC 0.68892E 01  CS 0.86318E 02 VG 0.83046E 00 CVG 0.12798E-02 CF 0.60446E 02

T 0.11200E 02   VBP 0.78308E 00 DVP 0.19775E-04 VC 0.16142E-00 CVC-0.17164E-01 VB 0.83058E 00 OVB 0.94236E-02 VIN 0.25000E 01
                IE-0.26641E 02 HFE 0.85000E 02 RB 0.15000E-01 GD 0.39574E-00 GS 0.17333E 01 ID 0.90966E 02 CE 0.12998E 02
                CC 0.69248E 01  CS 0.95201E 02 VG 0.83058E 00 CVG 0.94236E-02 CF 0.66656E 02

T 0.11400E 02   VBP 0.78311E 00 DVP 0.10587E-03 VC 0.15822E-00 CVC-0.14955E-01 VB 0.83058E 00 OVB 0.12096E-02 VIN 0.25000E 01
                IE-0.26657E 02 HFE 0.85000E 02 RB 0.15000E-01 GD 0.39604E-00 GS 0.18780E 01 ID 0.91037E 02 CE 0.13002E 02
                CC 0.69564E 01  CS 0.10377E 03 VG 0.83058E 00 CVG 0.12096E-02 CF 0.72687E 02

T 0.11600E 02   VBP 0.78313E 00 OVP-0.68890E-05 VC 0.15541E-00 CVC-0.13222E-01 VB 0.83068E 00 OVB 0.96776E-02 VIN 0.25000E 01
                IE-0.26685E 02 HFE 0.85000E 02 RB 0.15000E-01 GD 0.39630E-00 GS 0.20151E 01 ID 0.91118E 02 CE 0.13007E 02
                CC 0.69848E 01  CS 0.11204E 03 VG 0.83068E 00 CVG 0.96776E-02 CF 0.78535E 02

T 0.11800E 02   VBP 0.78315E 00 OVP 0.83159E-04 VC 0.15293E-00 CVC-0.11686E-01 VB 0.83066E 00 OVB 0.13112E-02 VIN 0.25000E 01
                IE-0.26697E 02 HFE 0.85000E 02 RB 0.15000E-01 GD 0.39661E-00 GS 0.21445E 01 ID 0.91174E 02 CE 0.13011E 02
                CC 0.70104E 01  CS 0.11998E 03 VG 0.83066E 00 CVG 0.13112E-02 CF 0.84179E 02

T 0.12000E 02   VBP 0.78317E 00 OVP-0.37350E-04 VC 0.15073E-00 CVC-0.10493E-01 VB 0.83077E 00 OVB 0.10677E-01 VIN 0.25000E 01
                IE-0.26722E 02 HFE 0.85000E 02 RB 0.15000E-01 GD 0.39691E-00 GS 0.22667E 01 ID 0.91245E 02 CE 0.13015E 02
                CC 0.70335E 01  CS 0.12760E 03 VG 0.83077E 00 CVG 0.10677E-01 CF 0.89627E 02

T 0.12200E 02   VBP 0.78319E 00 OVP 0.10276E-03 VC 0.14875E-00 CVC-0.93393E-02 VB 0.83069E 00 OVB-0.17453E-02 VIN 0.25000E 01
                IE-0.26728E 02 HFE 0.85000E 02 RB 0.15000E-01 GD 0.39708E-00 GS 0.23822E 01 ID 0.91285E 02 CE 0.13018E 02
```

```
T 0.15600E 02   VBP 0.78333E 00 DVP-0.13316E-03  VC 0.13245E-00 DVC-0.24254E-02  VB 0.83107E 00 DVB 0.13303E-01 VIN 0.25000E 01
                IE-0.26874E 02 HFE 0.85000E 02  RB 0.15000E-01  GD 0.39918E-00  GS 0.35892E 01  CD 0.91785E 02  CE 0.13049E 02
                CC 0.72415E 01  CS 0.21779E 03  VG 0.83107E 00 DVG 0.13303E-01  CF 0.15591E 03

T 0.15800E 02   VBP 0.78334E 00 DVP-0.35844E-04  VC 0.13201E-00 DVC-0.22024E-02  VB 0.83109E 00 DVB 0.48931E-02 VIN 0.25000E 01
                IE-0.26869E 02 HFE 0.85000E 02  RB 0.15000E-01  GD 0.39920E-00  GS 0.36298E 01  CD 0.91790E 02  CE 0.13049E 02
                CC 0.72470E 01  CS 0.22080E 03  VG 0.83109E 00 DVG 0.48931E-02  CF 0.15817E 03

T 0.16000E 02   VBP 0.78334E 00 DVP-0.13610E-03  VC 0.13159E-00 DVC-0.21350E-02  VB 0.83108E 00 DVB 0.13332E-01 VIN 0.25000E 01
                IE-0.26862E 02 HFE 0.85000E 02  RB 0.15000E-01  GD 0.39929E-00  GS 0.36683E 01  CD 0.91813E 02  CE 0.13050E 02
                CC 0.72521E 01  CS 0.22366E 03  VG 0.83108E 00 DVG 0.13332E-01  CF 0.16032E 03

T 0.16200E 02   VBP 0.78334E 00 DVP-0.38408E-04  VC 0.13120E-00 DVC-0.19337E-02  VB 0.83111E 00 DVB 0.48977E-02 VIN 0.25000E 01
                IE-0.26876E 02 HFE 0.85000E 02  RB 0.15000E-01  GD 0.39930E-00  GS 0.37046E 01  CD 0.91816E 02  CE 0.13051E 02
                CC 0.72570E 01  CS 0.22637E 03  VG 0.83111E 00 DVG 0.48977E-02  CF 0.16237E 03

T 0.16400E 02   VBP 0.78335E 00 DVP-0.13864E-03  VC 0.13083E-00 DVC-0.18872E-02  VB 0.83110E 00 DVB 0.13347E-01 VIN 0.25000E 01
                IE-0.26888E 02 HFE 0.85000E 02  RB 0.15000E-01  GD 0.39939E-00  GS 0.37390E 01  CD 0.91837E 02  CE 0.13052E 02
                CC 0.72615E 01  CS 0.22894E 03  VG 0.83110E 00 DVG 0.13347E-01  CF 0.16431E 03

T 0.16600E 02   VBP 0.78335E 00 DVP-0.40707E-04  VC 0.13049E-00 DVC-0.17036E-02  VB 0.83112E 00 DVB 0.49016E-02 VIN 0.25000E 01
                IE-0.26883E 02 HFE 0.85000E 02  RB 0.15000E-01  GD 0.39940E-00  GS 0.37715E 01  CD 0.91839E 02  CE 0.13052E 02
                CC 0.72658E 01  CS 0.23138E 03  VG 0.83112E 00 DVG 0.49016E-02  CF 0.16616E 03

T 0.16800E 02   VBP 0.78336E 00 DVP-0.14080E-03  VC 0.13017E-00 DVC-0.16744E-02  VB 0.83110E 00 DVB 0.13361E-01 VIN 0.25000E 01
                IE-0.26894E 02 HFE 0.85000E 02  RB 0.15000E-01  GD 0.39948E-00  GS 0.38022E 01  CD 0.91858E 02  CE 0.13053E 02
                CC 0.72698E 01  CS 0.23370E 03  VG 0.83110E 00 DVG 0.13361E-01  CF 0.16791E 03

T 0.17000E 02   VBP 0.78336E 00 DVP-0.42521E-04  VC 0.12986E-00 DVC-0.15054E-02  VB 0.83112E 00 DVB 0.49009E-02 VIN 0.25000E 01
                IE-0.26888E 02 HFE 0.85000E 02  RB 0.15000E-01  GD 0.39948E-00  GS 0.38312E 01  CD 0.91858E 02  CE 0.13053E 02
                CC 0.72736E 01  CS 0.23590E 03  VG 0.83112E 00 DVG 0.49009E-02  CF 0.16958E 03

T 0.17200E 02   VBP 0.78336E 00 DVP-0.14247E-03  VC 0.12958E-00 DVC-0.14904E-02  VB 0.83111E 00 DVB 0.13360E-01 VIN 0.25000E 01
                IE-0.26899E 02 HFE 0.85000E 02  RB 0.15000E-01  GD 0.39956E-00  GS 0.38507E 01  CD 0.91877E 02  CE 0.13054E 02
                CC 0.72772E 01  CS 0.23799E 03  VG 0.83111E 00 DVG 0.13360E-01  CF 0.17116E 03

T 0.17400E 02   VBP 0.78336E 00 DVP-0.44171E-04  VC 0.12931E-00 DVC-0.13339E-02  VB 0.83113E 00 DVB 0.48959E-02 VIN 0.25000E 01
                IE-0.26893E 02 HFE 0.85000E 02  RB 0.15000E-01  GD 0.39956E-00  GS 0.38847E 01  CD 0.91876E 02  CE 0.13054E 02
                CC 0.72805E 01  CS 0.23997E 03  VG 0.83113E 00 DVG 0.48959E-02  CF 0.17267E 03

T 0.17600E 02   VBP 0.78337E 00 DVP-0.14394E-03  VC 0.12906E-00 DVC-0.13310E-02  VB 0.83112E 00 DVB 0.13348E-01 VIN 0.25000E 01
                IE-0.26904E 02 HFE 0.85000E 02  RB 0.15000E-01  GD 0.39963E-00  GS 0.39094E 01  CD 0.91893E 02  CE 0.13055E 02
                CC 0.72837E 01  CS 0.24186E 03  VG 0.83112E 00 DVG 0.13348E-01  CF 0.17410E 03

T 0.17800E 02   VBP 0.78337E 00 DVP-0.45540E-04  VC 0.12883E-00 DVC-0.11848E-02  VB 0.83114E 00 DVB 0.48923E-02 VIN 0.25000E 01
                IE-0.26897E 02 HFE 0.85000E 02  RB 0.15000E-01  GD 0.39962E-00  GS 0.39326E 01  CD 0.91892E 02  CE 0.13055E 02
                CC 0.72866E 01  CS 0.24364E 03  VG 0.83114E 00 DVG 0.48923E-02  CF 0.17545E 03

T 0.18000E 02   VBP 0.78337E 00 DVP-0.14506E-03  VC 0.12861E-00 DVC-0.11920E-02  VB 0.83113E 00 DVB 0.13339E-01 VIN 0.25000E 01
                IE-0.26908E 02 HFE 0.85000E 02  RB 0.15000E-01  GD 0.39969E-00  GS 0.39547E 01  CD 0.91908E 02  CE 0.13056E 02
                CC 0.72895E 01  CS 0.24533E 03  VG 0.83113E 00 DVG 0.13339E-01  CF 0.17674E 03

T 0.18200E 02   VBP 0.78337E 00 DVP-0.46737E-04  VC 0.12840E-00 DVC-0.10548E-02  VB 0.83115E 00 DVB 0.48869E-02 VIN 0.25000E 01
                IE-0.26901E 02 HFE 0.85000E 02  RB 0.15000E-01  GD 0.39968E-00  GS 0.39755E 01  CD 0.91905E 02  CE 0.13056E 02
                CC 0.72921E 01  CS 0.24694E 03  VG 0.83115E 00 DVG 0.48869E-02  CF 0.17796E 03

T 0.18400E 02   VBP 0.78337E 00 DVP-0.14603E-03  VC 0.12820E-00 DVC-0.10706E-02  VB 0.83113E 00 DVB 0.13324E-01 VIN 0.25000E 01
                IE-0.26911E 02 HFE 0.85000E 02  RB 0.15000E-01  GD 0.39974E-00  GS 0.39953E 01  CD 0.91921E 02  CE 0.13057E 02
                CC 0.72946E 01  CS 0.24847E 03  VG 0.83113E 00 DVG 0.13324E-01  CF 0.17913E 03

T 0.18600E 02   VBP 0.78338E 00 DVP-0.47855E-04  VC 0.12802E-00 DVC-0.94118E-03  VB 0.83115E 00 DVB 0.48801E-02 VIN 0.25000E 01
                IE-0.26904E 02 HFE 0.85000E 02  RB 0.15000E-01  GD 0.39973E-00  GS 0.40139E 01  CD 0.91918E 02  CE 0.13057E 02
                CC 0.72969E 01  CS 0.24991E 03  VG 0.83115E 00 DVG 0.48801E-02  CF 0.18022E 03

T 0.18800E 02   VBP 0.78338E 00 DVP-0.14689E-03  VC 0.12784E-00 DVC-0.96428E-03  VB 0.83114E 00 DVB 0.13305E-01 VIN 0.25000E 01
                IE-0.26914E 02 HFE 0.85000E 02  RB 0.15000E-01  GD 0.39979E-00  GS 0.40316E 01  CD 0.91933E 02  CE 0.13058E 02
```

A NONLINEAR TRANSISTOR MODEL AND DEVICE CHARACTERIZATION

by

PARVIZ KIANKHOOY-FARD

B. S., Missouri University, 1963

AN ABSTRACT OF A MASTER'S REPORT

submitted in partial fulfillment of the

requirements for the degree

MASTER OF SCIENCE

Department of Electrical Engineering

KANSAS STATE UNIVERSITY
Manhattan, Kansas

1966

An approach to transistor transient and steady state prediction for large signal, small signal, and both large signal and small signal simultaneously is described which uses a nonlinear equivalent circuit model. The model is based on the Eber and Moll's equations (intrinsic model). The model is modified by introducing extrinsic elements. The model is further completed by further investigation of collector junction under forward biased condition. A comparison of experimental and predicted results are presented for a saturated inverter circuit, an emitter-follower, and a three stage d-c coupled amplifier. The method of device characterization is outlined in detail. A sensitivity study is performed, and the relative sensitivity of the device parameter is pointed out. Theoretical results are obtained from numerics solution of a system of nonlinear differential equations describing the model and circuit diagram. The nature of the errors in the program are pointed out. The capability of the model to linear amplifier design is discussed and an integrated switching and linear amplifier specification is proposed. A subroutine program is proposed, which will enable the circuit designer to handle the transistor as one would have handled such circuit elements as the resistor, or the capacitor in a circuit without much knowledge about the material of the resistor or the capacitor.